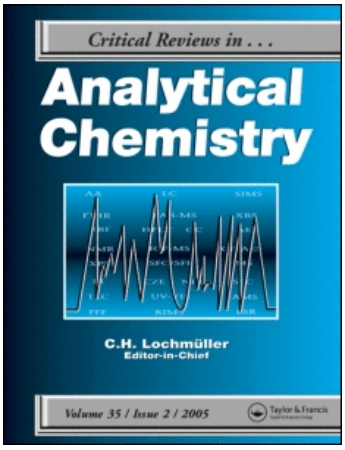

Critical Reviews in Analytical Chemistry
Publication details, including instructions for authors and subscription information:
http://www.informaworld.com/smpp/title~content=t713400837

Potentiometric Stripping Analysis: A Review

J. M. Estela[a]; C. Tomás[a]; A. Cladera[a]; V. Cerdà[a]
[a] Department of Chemistry, University of Balearic Islands, Palma de Mallorca, Spain

To cite this Article Estela, J. M. , Tomás, C. , Cladera, A. and Cerdà, V.(1995) 'Potentiometric Stripping Analysis: A Review', Critical Reviews in Analytical Chemistry, 25: 2, 91 — 141
To link to this Article: DOI: 10.1080/10408349508050559
URL: http://dx.doi.org/10.1080/10408349508050559

Critical Reviews in Analytical Chemistry, 25(2):91–141 (1995)

Potentiometric Stripping Analysis: A Review

J. M. Estela, C. Tomás, A. Cladera, and V. Cerdà

Department of Chemistry, University of Balearic Islands, 07071 Palma de Mallorca, Spain

ABSTRACT: A bibliographic review (150 references) on potentiometric stripping analysis (PSA) is performed. Theoretical, instrumental, analytical applications and advantages, and inferences of other modern PSA techniques are considered, like derivative PSA, constant-current PSA, multichannel potentiometric monitoring stripping analysis, differential PSA, constant-current enhanced PSA, derivative adsorptive PSA, kinetic PSA and reductive PSA.

Implementation of PSA in flow systems is also considered, namely continuous-flow and flow-injection systems.

KEY WORDS: potentiometric stripping analysis (PSA), background, instrumentation, applications, flow systems, continuous flow, flow injection analysis.

I. INTRODUCTION

In 1976, Jagner and Graneli[1] reported a novel analytical technique for the determination of metal traces that they called potentiometric stripping analysis (PSA) because analyses based on the oxidation of species previously deposited on an electrode by oxidants carried convectively to the electrode surface had not yet been included among electroanalytical techniques by the International Union of Pure and Applied Chemists (IUPAC). However, as admitted by its proponents themselves, the technique should be referred to more accurately as *chronopotentiometric stripping analysis*. This technical alternative arose from polarographic methods (more specifically, from anodic stripping voltammetry, ASV). In both techniques, metals in a sample are electrolytically concentrated by deposition on an electrode (usually a rotating mercury film electrode) prior to analysis proper. The two, however, differ in the way deposited metals are stripped and the analytical signal is obtained. In ASV, stripping is done electrochemically (Figure 1) by applying a usually linear potential scan to the working electrode over a given period during which the current circulating by the electrode is recorded as a function of the applied potential. When such a potential equals the oxidation potential of one of the deposited metals, the metal in question is stripped from the electrode, which is accompanied by an increase in the measured current. Each metal is thus identified by the presence of a maximum in the current/potential recording obtained, as the position of the maximum (E_p) is characteristic of each metal and its height (i_p) is proportional to the metal concentration in solution. The signal is overlapped with a non-Faradic background current originating from the electric charge at the electrode-solution interface, which is the greatest hurdle to be overcome in order to lower determination limits. The effect of such a current can be lessened by using several variants of ASV based on the application of nonlinear potential ramps; such variants include alternate

1040-8347/95/$.50

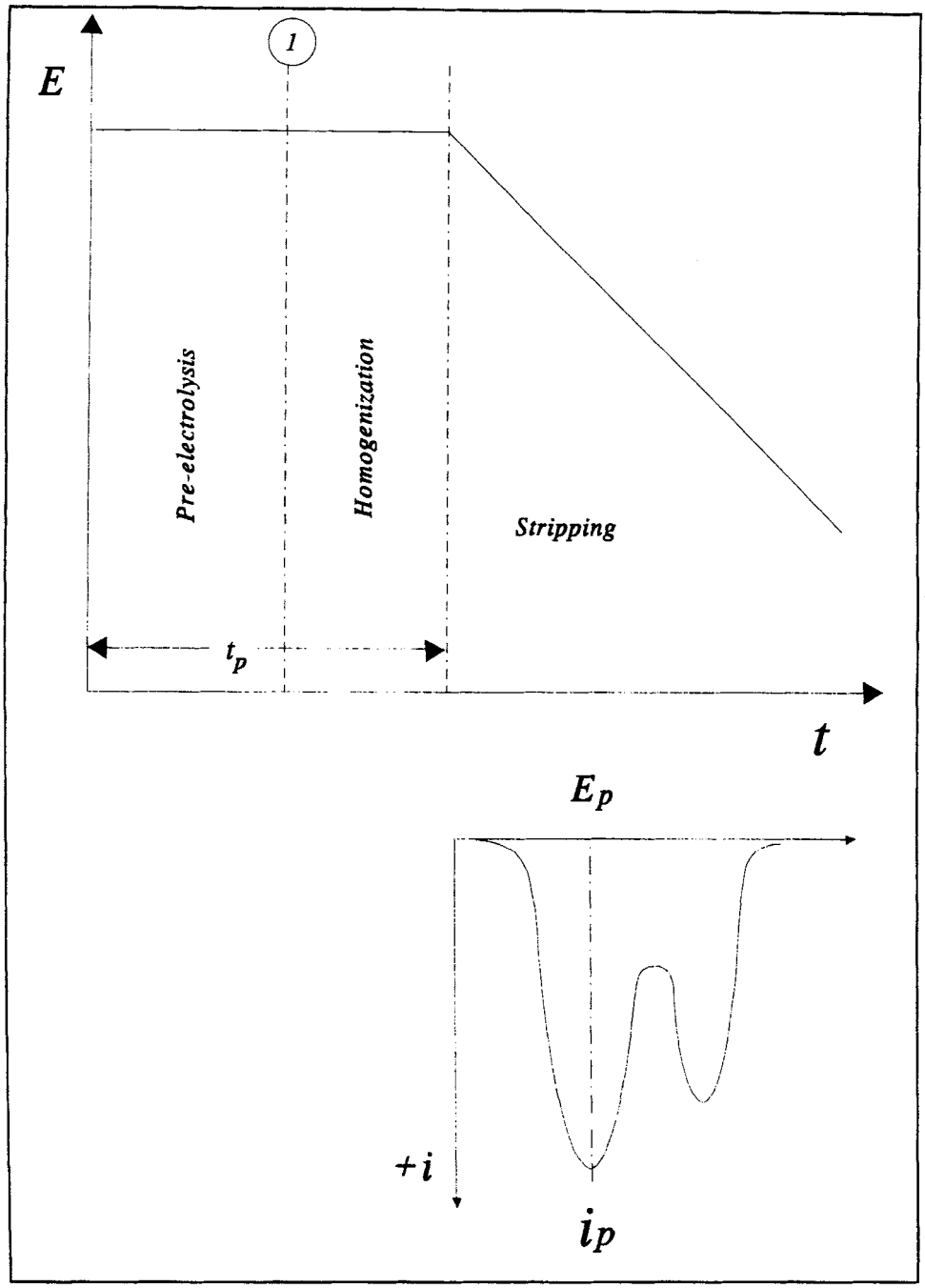

FIGURE 1. Timing of anodic stripping voltametry analysis.

current ASV (acASV) and differential pulse ASV (dpASV), which provide substantially improved detection limits.

In PSA, however, no control is made of the potential of the working electrode during metal stripping (Figure 2), which is accomplished by using a chemical oxidant in solution — usually Hg(II) or dissolved oxygen. The working conditions are set in such a way that the rate of oxidation of deposited metals remains constant throughout the stripping process; such a rate is determined by that of oxidant diffusion from the solution to the electrode surface. Under these condi-

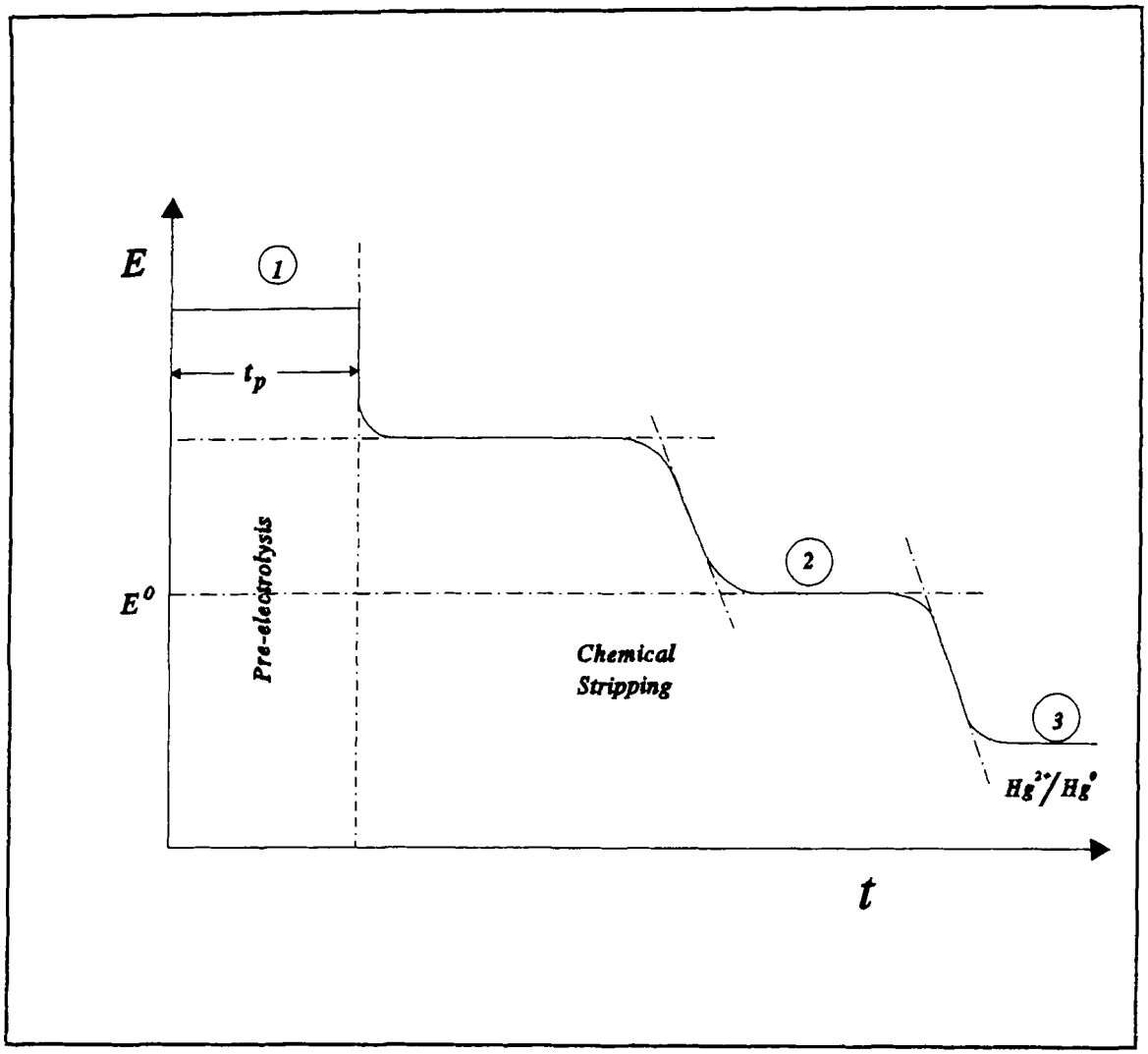

FIGURE 2. Timing of potentiometric stripping analysis.

tions, the analytical signal is recorded by monitoring the potential of the working electrode as a function of time. The curves thus obtained can be interpreted as being provided by a redox titration of deposited metals in which the titrant is added over them at a constant rate. The distance between the two consecutive equivalence points in a curve will be proportional to the metal concerned in solution, whereas the potential of the central zone (E^0) will be characteristic of it.

The most salient feature of stripping techniques is that dissolved metals concentrate at the working electrode during the electrodeposition step (zone 1), thereby substantially lowering their detection limits. In addition, the sensitivity can be adjusted to the particular requirements by choosing an appropriate electrodeposition time. The PSA technique is comparable to ASV in terms of sensitivity but lags slightly behind acASV and dpASV in this respect.[2] On the other hand, it features several major advantages over voltammetric techniques:

1. Potentiometric stripping can be implemented by using straightforward equipment such as a three-electrode cell, a

high-impedance operational amplifier, an x/t recorder, and a potentiostat. Use of the potentiostat can be simplified to operating at a single potential (e.g., −1.25 V vs. SCE, where all metals suitable for analysis will be reduced and hydrogen formation avoided). In addition, times can be measured more readily and precisely than microcurrents and no potential ramp need be used (in contrast with ASV), which results in diminished instrumental costs.

2. Both ASV and PSA are multielement techniques. The width of ASV bands and hence discrimination between different elements is a function of the analyte concentration and the potential scan rate. This somehow complicates the analysis of samples containing rather different concentrations of the species to be determined because adequate resolution can only be achieved by applying a slow potential ramp (which lengthens analyses) or altering the scan rate during stripping. Because the electrode potential in PSA is controlled by an oxidation process, the "scan rate" is self-optimized, so signal discrimination is more than adequate whatever the analyte concentration ratios. This, however, has one major limitation. Because the electrode potential remains virtually constant during stripping until the analyte concerned is depleted, those elements being deposited at the potential in question will continue to be deposited until the analyte is fully stripped. The end result is that the signal for an element depends, however slightly, on the concentration of the elements that are stripped before it.
3. Potentiometric stripping analysis has proved to be feasible in samples with ionic strengths down to 10^{-4} *M*, as well as polar organic solvents such as propanol and acetic acid, and in the presence of electroactive organic species provided they are not deposited on (and hence do not alter) the electrode or change the rate of oxidation of deposited elements. In contrast to ASV, no current is drawn through the sample during the stripping phase.
4. The structure of the thin mercury film changes during preelectrolysis because of the sustained increase in film thickness. Frequently, the film is also affected by adsorbents or nitrogen bubbles. The net effect is that the transport rate of analytes into the mercury film differs slightly between the analysis of a sample as such and from a standard aliquot. In PSA, the rate of transport of oxidants is similarly affected, thus partly compensating for this effect. This also holds with changes in the electrode rotation rate. Neither effect is offset, for example, in ASV.
5. As in ASV, PSA signals overlap with a background signal due to charge currents at the electrode/solution interface. However, PSA background signals are less significant.
6. PSA has also proven suitable for the analysis of heavy metals at concentrations in the range 0.1 to 1.0 ppm, where no deaeration is required. The constant oxygen concentration in the sample can be advantageously used for oxidation during stripping. Due care should be exercised, however, that the analyte solubility in the mercury phase is not exceeded. In addition, samples must be buffered in the acid region during preelectrolysis in order to avoid the formation of insoluble or irreversible hydroxo species.

On the other hand, PSA also has several pitfalls, some of which are common to all techniques involving mercury film electrodes. Thus:

1. Like all other thin mercury film techniques, PSA is affected by the formation of intermetallic compounds. Thus, the 1:1 copper-zinc intermetallic compound poses severe interferences, which, however, can be overcome by the addition of gallium.
2. One unique disadvantage of PSA is the decrease in the oxidant concentration during preelectrolysis. This shortcoming can be circumvented by making the electrode surface small relative to the overall sample volume.
3. The analytical signals provided by mercury film electrodes are markedly influenced by the electrode's history. In PSA, the use of Hg(II) as the oxidant eliminates the risk of destroying the mercury film between consecutive analyses; during stripping, the potential of the working electrode will automatically stop before it reaches the region of mercury oxidation (zone 3 in Figure 2). Formation of, for example, calomel on the film surface, is thus hindered. Also, there is no risk of oxidation of the glassy carbon surface. Using an oxidant other than Hg(II) considerably increases the risk of the mercury film being destroyed, so that it must be regenerated more frequently. Fortunately, the electrode can be regenerated *in situ* if desired and analyses performed by using the standard-addition method.
4. Stripping analysis, both potentiometric and voltammetric, is particularly well suited to the determination of heavy metals in liquid samples, no pretreatment of which is often needed. The time-consuming step of analyses in such conditions is plating. This has made automating the technique mandatory. On the other hand, plating can be further expedited by using microprocessor-controlled units enabling rapid acquisition and processing of stripping data; use of such units has led to new PSA variants of improved sensitivity, selectivity, and expeditiously. The added use of continuous-flow and flow-injection systems for this purpose contributes to further increased throughput and selectivity.
5. One other major limitation of ASV and PSA is that direct stripping analyses with adequate sensitivity are only feasible for a small number of analytes. This is particularly true of PSA when dissolved oxygen is used as the oxidant. One way of extending application to a wider range of analytes entails improving deposition (whether anodic or cathodic) and/or the stripping step by using an electrode other than that of mercury film or an oxidant different from Hg(II) and dissolved oxygen, by altering the stripping solution or by using an alternative technique to record or process the analytical signal.

II. VARIANTS OF PSA TECHNIQUE

The PSA techniques can be classified into the following variants.

A. Derivative Potentiometric Stripping Analysis (dPSA)

This variant of PSA was developed by Jagner and Aren[2] in order to facilitate evaluation of the analytical signal by using its derivative. The signal is obtained in the same way as in conventional PSA. The dPSA technique involves preconcentrating metal analytes in a thin mercury film covering a glassy carbon electrode and subsequently measuring the electrode potential subject to controlled transport of oxidant to the electrode surface. After plating, the potential of the working electrode is recorded with the aid of an operational amplifier coupled as a voltage monitor. The time derivative of the

signal is registered on a second recorder channel by means of derivative circuitry. The dE/dt vs. t graph thus obtained (Figure 3) exhibits maxima at those points where a conventional PSA curve would show a sharp variation of the potential with time. The distance between two consecutive maxima corresponds to an analytical signal equivalent to the plateau length in conventional PSA but is easier to determine with a higher precision.

B. Constant-Current Stripping Analysis (CCSA)

Whereas some authors regard this technique as a variant of PSA,[3] others claim that it should be called "chronopotentiometric stripping analysis".[2] In this technique, the metal analyte is stripped by a constant oxidizing current passed through the working electrode rather than by a chemical oxidant. In both PSA and CCSA, the time needed for the analyte to be oxidized is directly proportional to the metal ion concentration (Figure 4). This technique has been used intensively by Renman et al.[4] in flow systems, as well as in some special applications, including the determination of lead in gasoline[5] and the use of polymer-modified electrodes.[3] As in voltammetry,[6] passing an electric current during stripping gives rise to interferences from electroactive species present in samples; such interferences, however, can readily be overcome, particularly in flow systems, by subjecting a matrix other than that of the sample to stripping (i.e., using the matrix-exchange technique) or employing a physically or chemically modified electrode.

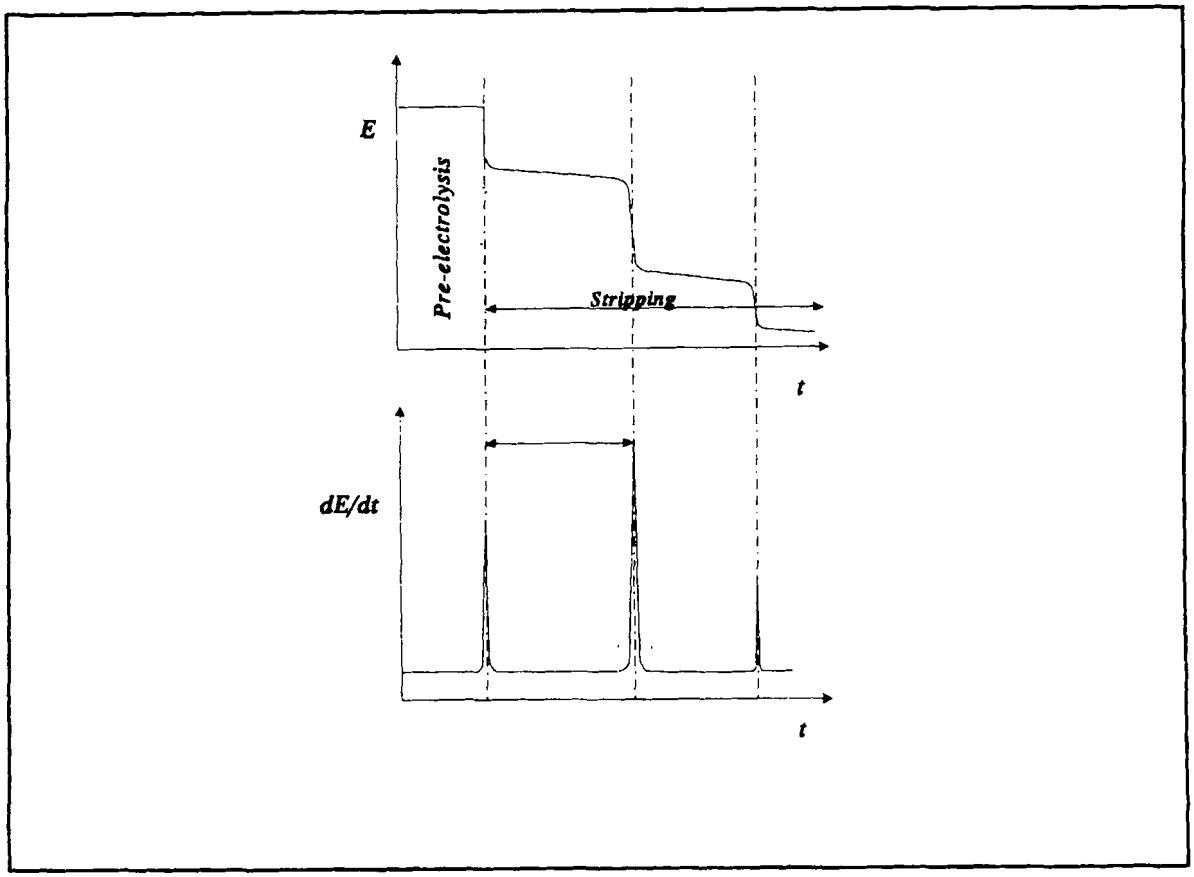

FIGURE 3. Timing of derivative potentiometric stripping analysis.

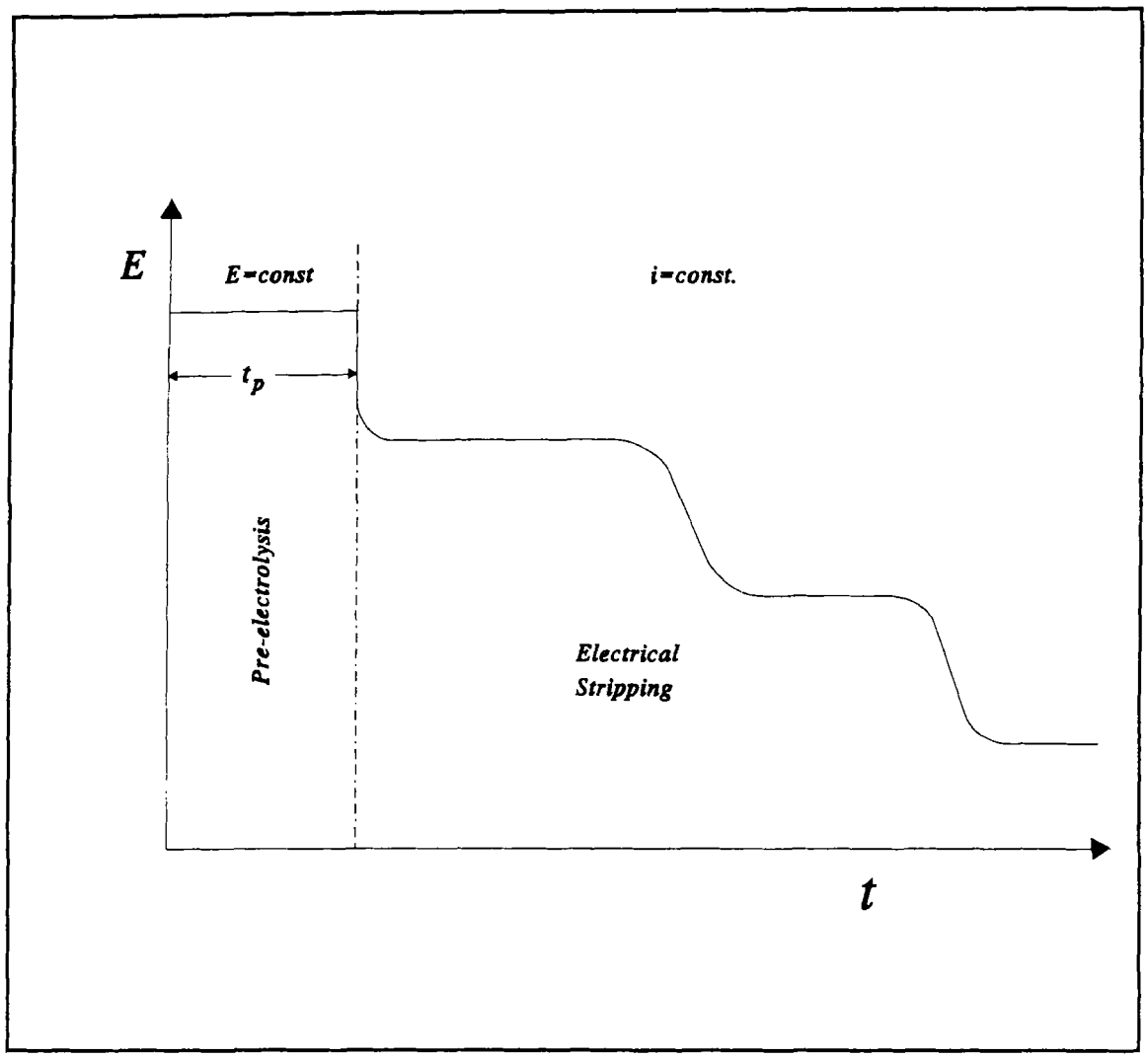

FIGURE 4. Timing of constant current stripping analysis.

C. Multichannel Potentiometric Monitoring Stripping Analysis (MSPSA)

This technique was originally developed and subsequently used intensively by Mortensen et al.[7] The stripping time is electrochemically enhanced by using a computerized data acquisition technique, viz., multichannel potentiometric monitoring (Figure 5) in conjunction with potentiometric stripping analysis (MSPSA). After a single, short deposition period, a substantial fraction of the accumulated metal may be forced to undergo several oxidations and rereductions in a precisely timed sequence. The computer acquires and adds up the analytical signals, viz., the number of time units (clock pulses) resulting from the oxidation steps within the preselected potential window. Thus, even after a short plating period, a relatively small amount of preconcentrated metal may produce a significant analytical signal. The feasibility of enhancing signals by using computerized multiscanning in conjunction with voltammetric stripping analysis has been demonstrated beyond doubt. The extent to which the analytical signal can be enhanced depends heavily on how efficiently freshly oxidized metals can be recov-

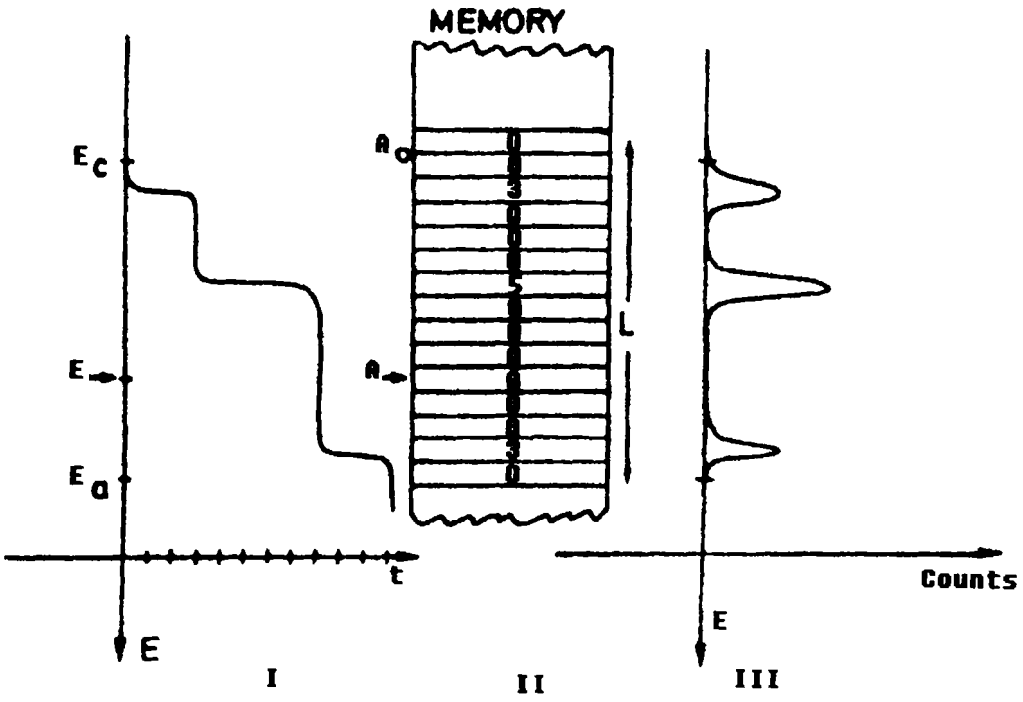

FIGURE 5. (I) Potential vs. time behavior of working electrode during redissolution of three amalgamated metals. $E_a - E_c$ is the potential window studied. (II) Computer memory section: the data storage area starting at address A_0 holds a record of accumulated clock pulse counts. (III) The resultant multichannel potentiogram. (From Mortensen, J.; Ouziel, E.; Skov, H. J.; Kryger, L. *Anal. Chim. Acta.* **1979,** *112,* 297–312. With permission.)

ered (rereduced) after each cyclic scan. If the time available for oxidized metal to escape from the working electrode by diffusion in a quiet solution is short, its recovery will be quite high. Optimal signal enhancement can be achieved by using fast anodic scans; the oxidation potential is scanned only as far as required to obtain the signal, and this is followed by a prompt return to the reduction potential. Similarly, in multiscanning PSA, chemical oxidation should proceed rapidly, followed by resumption of potentiostatic control at the reduction potential. As in potentiometric stripping, the rate of the oxidation process may be controlled by the amount of oxidant added to the solution; a high recovery of metals can be expected if a proportionally large excess of oxidant is used. This technique is suitable for stripping analysis with preconcentration times of 60 to 90 s at a mercury film electrode and provides linear responses from 1 to 100 μg/l Cd(II) and Pb(II). The detection limit falls to ~5 ng/l for a preconcentration time of 30 min.

D. Differential Potentiometric Stripping Analysis (DPSA)

This is a computer-assisted variant of PSA originally developed by Kryger.[8] In DPSA, as in PSA, stripping of preconcentrated analytes is caused by some oxidant in the sample solution being transported to the working electrode, and the process is recorded potentiometrically. If the rate of stripping is high relative to that at which the

newly stripped material can escape (by diffusion or convection) from the vicinity of the working electrode, a high concentration region of analyte is created around the working electrode during the stripping step. The DPSA technique exploits the formation of such a region: after plating is finished, potentiostatic control is stopped and the potential of the working electrode is recorded as a function of time with the aid of a microcomputer. The electrode potential is (Figure 6), however, allowed to undergo only a small change ($\Delta E' \simeq 10$ to 50 mV) and, as soon as a preset potential threshold is reached, potentiostatic conditions are resumed over a short period at a plating potential slightly anodic of the previous one, ΔE. In this way, a substantial amount of newly oxidized material can be replated and reoxidized in a subsequent stripping step going from the new plating potential across the selected potential window. The procedure is repeated until the entire potential range of interest has been covered. With a suitable choice of potential windows, the stripping signal at any potential interval is recorded several times and the results are accumulated in the computer memory. Hence, for a given plating period, a signal enhancement is likely to result. The process is analogous to the multiscanning effect that provides the increased sensitivity of differential pulse stripping voltammetry relative to the linear sweep technique. The differential potentiogram obtained is essentially the derivative of time with respect to potential, and where the stripping potentiogram exhibits a plateau signalling the stripping of a component, the differential potentiogram shows a maximum (Figure 6). The signals for trace elements such as cadmium and lead, which exhibit transport-controlled potentiometric stripping, can be enhanced by using a scheme involving multiple stripping and rereduction of preconcentrated analytes, the detection limits for which are below 5×10^{-10} *M* if a 60-s plating time is

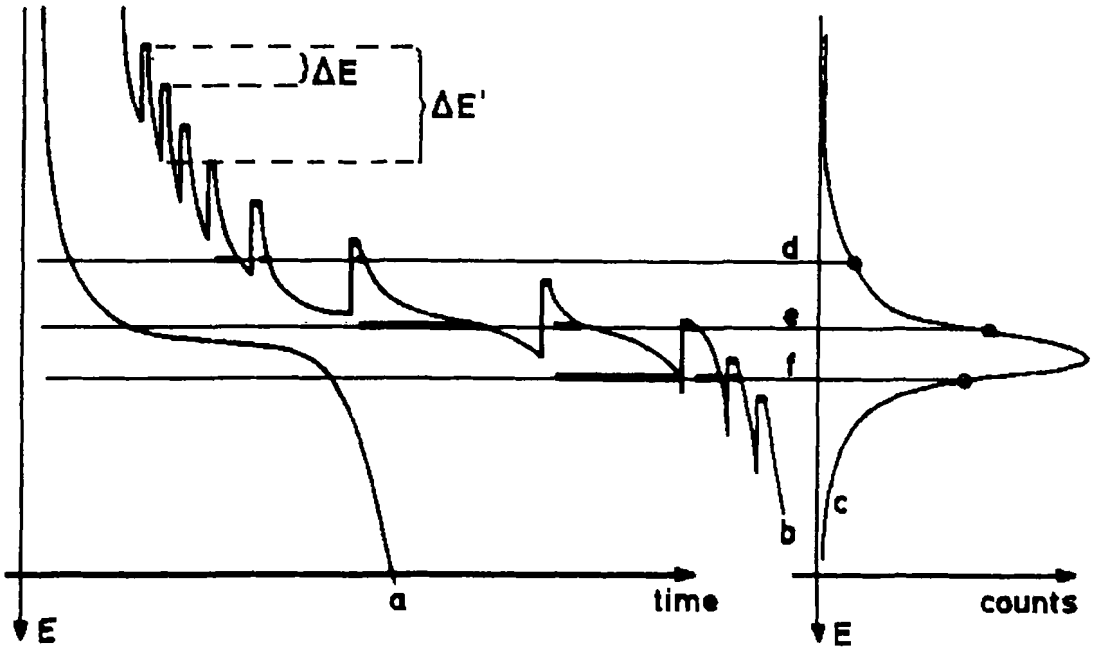

FIGURE 6. Principle of differential potentiometric stripping analysis. Curve a, normal potential vs. time behavior during stripping of a plated component; curve b, potential vs. time behavior during differential potentiometric stripping; curve c, differential stripping potentiogram. (From Kryger, L.; *Anal. Chim. Acta.* **1980,** *120,* 10–30. With permission.)

used. The accuracy of this technique was tested on a biological reference material. Like PSA, the DPSA technique is insensitive to reversible redox couples present in solution.

The technique is somehow related to multiscanning PSA; however, the latter uses a single plating potential and the potential interval for each scan is on the order of several hundred millivolts, so cadmium and lead, for example, may be stripped in the same scan. This results in an unwanted correlation of the cadmium recovery with the lead concentration: a high concentration of lead forces the working electrode to remain at the stripping potential of lead for a long time. At such a potential, newly stripped cadmium can escape from the working electrode by diffusion-convection, so there will be a poor recovery of this metal between scans. In DPSA, the magnitude of $\Delta E'$ is kept sufficiently small, so cadmium and lead are not stripped in the same scan and the previous correlation vanishes. The correlation problem in the multiscanning technique is overcome by allowing the magnitude of the stripping interval to increase gradually. Thus, the component with the most cathodic stripping potential is determined by multiple scanning; then, another component is included in the scan, and so on. This "interrupted stripping" can be considered a crude type of DPSA, but requires prior knowledge of the stripping potentials involved. Also, achieving substantial analyte recoveries in multiscanning potentiometric analysis entails stripping in a quiet solution, which is unnecessary with DPSA.

E. Constant-Current-Enhanced Potentiometric Stripping Analysis (CCEPSA)

In this technique, a constant cathodic current is applied to the electrode system during the chemical stripping step in order to force freshly stripped analyte to be redeposited into the mercury film. Some of the stripped species undergo several "oxidation-reduction" cycles, so the stripping time is extended. Zie and Huber[9] used rotating mercury film electrodes, Cd(II) during stripping and dissolved oxygen as oxidant to develop and thoroughly test this technique, the foundation of which is inspired by catalytic stripping as applied to ASV and CCSA in order to improve the sensitivity. The cathodic catalysis process is very strongly influenced by the prevailing hydrodynamic conditions. In order to achieve the maximum possible catalytic effect, stripping should be carried out in a quiet solution so as to ensure the formation of a high concentration zone of freshly stripped analyte in the vicinity of the electrode surface. The CCEPSA technique is more sensitive than conventional PSA by at least one order of magnitude. This enhancing factor is equally applicable to CCEPSA detection limits. Figure 7 shows some typical stripping curves for Cd(II) obtained by using this technique.

F. Derivative Adsorptive Potentiometric Stripping Analysis (dAPSA)

This technique, another variant of PSA, was originally developed by Jin and Wang,[10] who called it "derivative adsorption stripping potentiometry". The dAPSA technique was conceived to extend the application of PSA to organic compounds and some inorganic elements (e.g., iron, cobalt, and nickel) that cannot be electrolytically preconcentrated on mercury. It exploits the adsorptive capacity of some organic compounds and inorganic complexes to preconcentrate them at an electrode. The adsorbed compounds are subsequently stripped by the effect of an oxidant or reductant. The process involves the following reactions:

$$O_{sol} \rightleftharpoons O_{ads} \quad (1)$$

$$O_{ads} + ne^- \rightleftharpoons R_{ads} \quad (2)$$

$$m\ R_{ads} + n'\ Ox \rightarrow m\ O_{ads} + n'\ Red \quad (3)$$

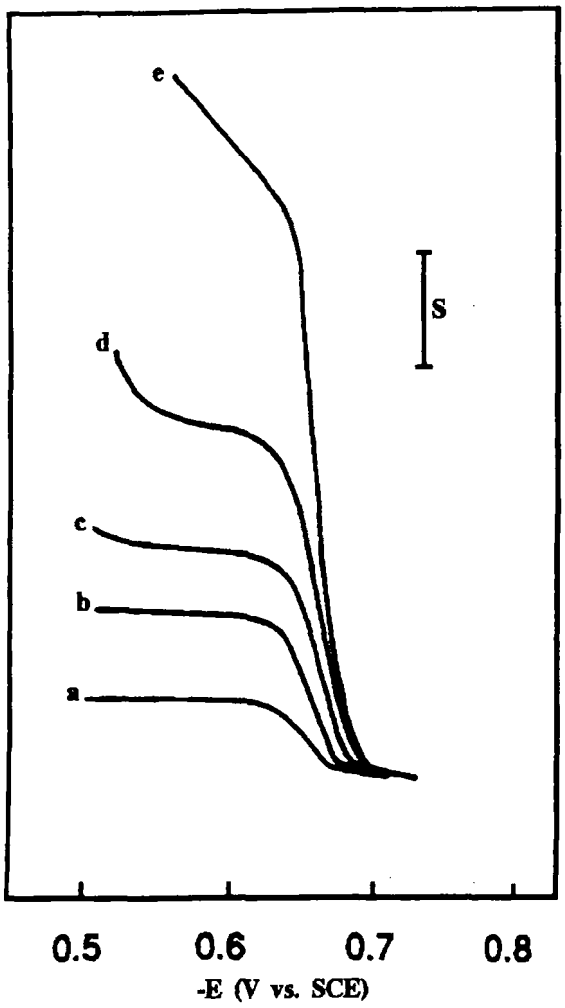

FIGURE 7. Effect of the imposed cathodic current on the shapes of the stripping curves. (a) 0; (b) 3.5; (c) 4.5; (d) 5; (e) 5.75 μA. 1.0×10^{-6} *M* Cd^{2+} in pH 5 acetate buffer; deposition time (t_d) 2.0 min; deposition potential (E_d) –0.9 V vs. SCE. S = 4.8 s for curves a, b, c, and d and 20 s for curve e. (From Zie, Y.; Huber, C. O.; *Anal. Chim. Acta.* **1992,** *263,* 63–70. With permission.)

where O and R denote oxidized and reduced species, respectively; the subscripts sol and ads the solution phase and adsorption phase, respectively; and Ox the oxidant and Red its reaction product.

Potential (E) and time (t) data are digitized, converted to dt/dE values, and plotted against the potential, which results in increased sensitivity and resolution. The technique is applicable to quiet and stirred solutions alike. Equations for the reversible process involved were derived and tested by using 1-hydroxyanthraquinone as analyte and Hg(II) as oxidant in deaerated solutions.

G. Kinetic Potentiometric Stripping Analysis (KPSA)

This automated variant of PSA originated from the findings of Cladera et al.[11] in studying various oxidants and working electrodes for the determination of mercury by PSA. They found the shape of the stripping curves for mercury deposited on a gold electrode by using the periodate/iodide system as oxidant to deviate from conventional PSA curves and resemble kinetic profiles more closely (Figure 8). Pertinent calibration curves can therefore be constructed by using ordinary kinetic treatment methods such as those of the initial rate and fixed potential.

The overall process can be interpreted as follows: in the electrolysis step, mercury is reduced on the gold surface, with which it amalgamates:

$$Hg^{2+} + 2\ e^- \rightarrow Hg(Au) \qquad (4)$$

When the amount of deposited mercury is large enough, a layer of unamalgamated mercury may also be formed in addition to the previous one. During stripping, the curve obtained on addition of periodate after preelectrolysis is consistent with a process in which mercury is either oxidized with a very slow kinetics or not oxidized at all. In the presence of iodide, addition of periodate to an acid medium results in the release of iodine, which gives rise to the kinetic curve for mercury oxidation through the following reaction:

$$Hg(Au) + I_2 + 2\ I^- \rightarrow HgI_4^{2-} \qquad (5)$$

When the amount of mercury present is quite large, the metal ion cannot penetrate the elec-

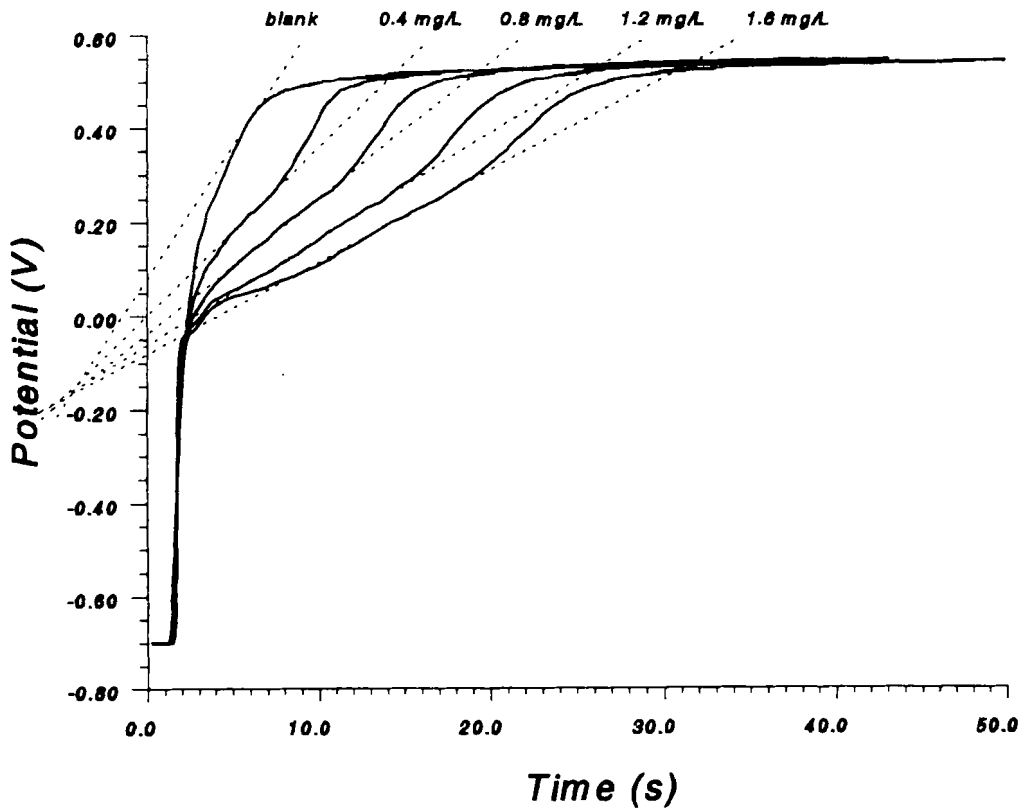

FIGURE 8. Kinetic potentiometric stripping analysis. Potentiograms obtained and slopes calculated at different Hg(II) concentrations. (From Cladera, A.; Estela, J. M.; Cerdà, V. *J. Electroanal. Chem.* **1990,** *288,* 99–109. With permission.)

trode completely, so, initially, the situation is equivalent to working with a pure mercury electrode; this gives rise to the typical plateau of PSA curves, the potential of which can be calculated by applying the Nernst equation to the HgI_4^{2-}/Hg system. Once the entire mercury surface is depleted or if the amount deposited is small enough to penetrate the gold electrode, the redox process may be limited by the kinetics of transfer from the bulk electrode to the interface. This phenomenon, together with slower transfer kinetics than those of the chemical oxidation reaction, accounts for the appearance of kinetic curves after the typical plateau (or even from the beginning of stripping if the amount of deposited mercury is rather small). This interpretation is supported by the fact that only the copperized graphite electrode gives rise to the expected plateau: that for copper followed by that for mercury. As the copper has already been stripped by the time the mercury is, the latter does not need to diffuse through the electrode, so it is only reoxidized in a step controlled by the chemical process and diffusion of the oxidant. The shape of the kinetic curves obtained, with two distinct slopes, can be explained by assuming the electrode potential to be determined first by the mercury concentration at the electrode surface, which in turn depends on its rate of diffusion through the gold. Once all the mercury has been oxidized, the slope changes again and becomes steeper as it reaches the plateau yielded by the blank.

H. Reductive Potentiometric Stripping Analysis (RPSA)

This modification of PSA was developed in order to extend application of con-

ventional PSA to those analytes that cannot be deposited cathodically owing to their low solubility in mercury or markedly cathodic half-wave reduction potentials. Such elements may occasionally be preconcentrated anodically and determined by cathodic stripping voltammetry. In addition, interferences may be overcome in some favorable cases by switching from anodic to cathodic stripping analysis. The RPSA technique was first implemented by Christensen and Kryger[12] using the determination of manganese as chemical model; the metal was preconcentrated by anodic oxidation at a platinum electrode and stripped by using hydroquinone as reductant (Figure 9). In this way, manganese was determined at concentrations in the microgram per milliliter range. The accuracy of the technique, tested on a standard biological material, is quite satisfactory.

In later work, Christensen et al.[13] demonstrated the suitability of amalgamated metals as reductants in RPSA. The amalgams were electrolytically generated from dissolved metals in a mercury pool. During stripping, the reductant, which was stored inside the working electrode, reacted with sparingly soluble mercury compounds of the analytes preconcentrated at the electrode surface (Figure 9). With amalgamated sodium, the technique proved to be suitable for the determination of selenium and sulfur at the 10^{-7} *M* level with a 1- to 2-min preconcentration. Halides can be determined at the 10^{-6} *M* level with a few seconds of preconcentration and use of a less powerful reductant such as amalgamated zinc.

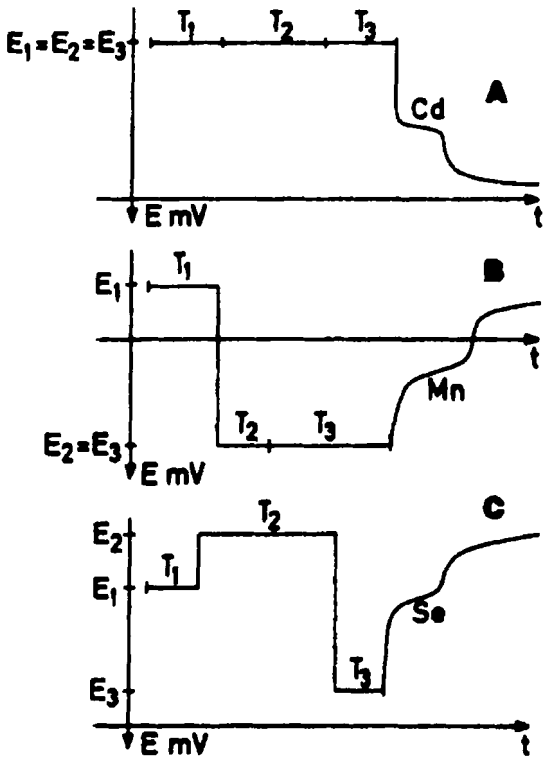

FIGURE 9. Time sequences of potentials generated during electrolysis by three-state potentiostat module. (A) Oxidative potentiometric stripping analysis. $T_1 + T_2 + T_3$ is the electrodeposition time. (B) Reductive potentiometric stripping analysis with water-soluble reducing agent. T2 + T3 is the electrodeposition time and T_1 is the electrode regeneration time. (C) Reductive potentiometric stripping analysis with electrolytical generated amalgamated metal as the reducing agent. T_1 is the electrode regeneration time, T_2 is the amalgam creation time, and T_3 is the electrodeposition time. (From Christensen, J. K.; Keiding, K.; Kryger, L.; Rasmussen, J.; Skov, H. J. *Anal. Chem.* **1981**, *53*, 1847–1851. With permission.)

III. THEORETICAL FOUNDATION OF POTENTIOMETRIC STRIPPING ANALYSIS

After the potentiostat is switched off once the electrodeposition of metals in a PSA experiment is finished, the potential of the working electrode rises rapidly until it reaches the nearest oxidation potential for the deposited metals. At this point, the metal in question is reoxidized and the potential remains virtually constant until the metal has been stripped completely. Then, the potential rises rapidly again until that of the next metal is reached. The process is repeated until all deposited metals have been stripped, after which the potential continues to rise until equilibrium with the bulk solution is reached.

As a result, each deposited metal gives rise to a horizontal segment (a "plateau") in the potential-time curve. The potential at which each plateau appears is characteristic of each metal and its length gives the time the metal takes to be oxidized. The rate at which each metal is oxidized is determined by the diffusion of the dissolved oxidant to the electrode, its oxidizing power, and the reaction kinetics. Consequently, it will depend on the nature and concentration of the oxidant, as well as the experimental conditions (stirring, nature and surface of the electrode, etc.).

The phenomena involved in the electrodeposition-stripping cycle at a mercury film electrode have been studied theoretically[14,15] in order to derive equations for the potential-time curves provided by the PSA technique.

During electrodeposition, the following generic reaction takes place at the electrode surface:

$$M_i^{n+} + n\,e^- \rightarrow M_i(Hg) \qquad (6)$$

where M_i^{n+} denotes the metal ions that can be reduced at the potential of the working electrode, the elemental forms of which are mercury soluble. If Equation 6 is rapid enough, the concentrations of metals in the vicinity of the electrode start to fall rapidly and a diffusion layer is established between the electrode surface and the bulk solution. On the other hand, because the electrodes have a fairly small surface, concentrations in the bulk solution can be assumed to remain constant throughout the experiment. Under these conditions, according to Fick's law of diffusion, the overall amount of metal that is deposited on the electrode over an interval t_{dep} is given by the following proportionality relationship:

$$M_i(Hg) \propto [M_i^{n+}] D_{Mi} t_{dep} \delta_1^{-1} S \qquad (7)$$

where $M_i(Hg)$ is the overall amount of deposited metal, $[M_i^{n+}]$ the metal concentration in the bulk solution, D_{Mi} the diffusion coefficient of the metal ion in solution, δ_1 the diffusion layer thickness during the electrodeposition time (t_{dep}), and S the effective surface area of the working electrode.

During stripping, the following generic reaction takes place:

$$M_i(Hg) + (n/m)\,A_j(ox) \rightarrow M_i^{n+} + (n/m)\,A_j(red) \qquad (8)$$

where A_j denotes the potential oxidants present in solution. Again, a diffusion layer is formed, only by A_j this time. On the assumption of rapid electrode reactions and the diffusion of A_j to the electrode as being the rate-determining step, the overall amount of A_j that reacts at the electrode during the stripping step can be expressed as

$$A_j(ox)_{tot} \propto [A_j(ox)] D_{Aj(ox)} \tau \delta_2^{-1} S \qquad (9)$$

where $[A_j(ox)]$ is the oxidant concentration in the bulk solution, $D_{Aj(ox)}$ its diffusion coefficient, τ the stripping time, and δ_2 the diffusion layer thickness during stripping. As in the previous case, concentrations in the bulk solution can be assumed to remain constant during stripping. A combination of Equations 7 and 9 yields an expression for the overall time required for the complete stripping of $M_i(Hg)$:

$$\tau_i \propto \frac{[M_i^{n+}] t_{dep} \delta_2 \delta_1^{-1}}{\sum \frac{n}{m_j} D_{A_j(ox)} [A_j(ox)]} \qquad (10)$$

according to which the signal obtained at a given metal concentration will increase with increasing electrodeposition time and decreasing concentration of oxidants in solution. On the other hand, the thicknesses of the diffusion layers formed during electrodeposition and stripping (δ_1 and δ_2, respectively) are directly related to the stirring of the solution in such steps. If stirring is

maintained constant in both steps, δ_1 and δ_2 will be virtually identical, so they can be eliminated from Equation 10. On the other hand, if stirring is stopped during stripping, δ_1 will be smaller than δ_2, so the signal will be increased as a result. However, this sensitivity-enhancing procedure is only recommended when a highly reproducible stirring system is available.

Finally, according to Equation 10, on constancy of the hydrodynamic conditions, oxidant concentration, and electrodeposition time, the signals obtained in a series of experiments will be proportional to the metal concentration in solution. This relationship is the basis for application of the PSA technique to quantitative analysis.

The equations above rely on the assumption that the rate-determining step of the process is the diffusion of species from the bulk solution to the electrode surface, which involves considering any processes potentially occurring in the thin mercury film formed on the electrode to have a negligible influence. However, such processes must be considered if an accurate equation for the potential-time curves is to be derived.

The potential of the working electrode at any time is given by the Nernst equation:

$$E = E^0 + \frac{RT}{nF} \ln\left(\frac{[M_i^{n+}]_s}{[M_i(Hg)]_s}\right) \qquad (11)$$

where $[M_i^{n+}]$ is the concentration of dissolved metal in the vicinity of the electrode and $[M_i(Hg)]_s$ that of amalgamated metal in the mercury layer at the electrode-solution interface. As a rule, as one of the metals, M_i, starts to be stripped, two diffusion layers are formed: one in the solution and the other in the mercury film covering the electrode. After a transition interval, a steady state is reached where concentrations at the electrode-solution interface, and hence the electrode potential, remain essentially constant until all deposited metal is stripped. On the assumption that diffusion in the mercury film on the electrode was the rate-determining step, Chau et al.[15] derived the following equation for the potential-time curve obtained from the metal stripping:

$$E = E^0 + \frac{RT}{nF} \ln\left(\frac{2l}{\pi\sqrt{D_0}}\right) + \frac{RT}{nF} \ln\left(\frac{\sqrt{t}}{\tau - t}\right) \qquad (12)$$

where l is the thickness of the mercury film covering the electrode, D_0 the diffusion coefficient for dissolved ions, and τ the time needed for deposited metal to be fully stripped.

So far, no mention has been made of electric bilayer phenomena at the electrode-solution interface. Such phenomena can be interpreted as the appearance of excess electronic charge at the electrode surface during application of the electrodeposition potential in order to counter the bilayer capacitance. When the potentiostat is switched off in order to start stripping, the excess electronic charge can give rise to the following generic reaction:

$$e^-_{exc} + (l/m_j)\, A_j(ox) \rightarrow (l/m_j)\, A_j(red) \qquad (13)$$

In contrast to the above reactions, where the potential is determined by electrons at well-defined energy levels, Equation 13 provides no constant-potential zones, but rather a semiexponential background signal that adds to the signal resulting from the stripping of the metals.

The literature abounds with theoretical studies aimed at elucidating, predicting, and checking for the phenomena involved in PSA. Mortensen and Britz[16] derived a model for predicting the background signal (E vs. t) in PSA and concluded that, in the absence of oxidizable materials at the working electrode, the E-t function is determined by the bilayer

capacity, which is strongly affected by dissolved surfactants.

Labar and Lamberts[17] demonstrated the feasibility of controlling the transport of oxidants to the surface of the working electrode (PSA at a stationary electrode) and found that, when linear diffusion of oxidizing species was the rate-determining step at the working electrode-solution interface and the physical properties of the medium were assumed to lower the diffusion coefficient of such species, the relative sensitivity of the technique was increased by a factor of 50 for all common ions assayed by PSA (Cu, Cd, Zn, Pb, Bi, Tl, and Ga).

Hussam and Coetzee[18] reported a theoretical treatment based on the assumption of an initial parabolic concentration gradient of the metal in mercury and stripping in a stirred solution, which is the usual condition for PSA. They derived and experimentally validated equations for the transient potential as a function of time, as well as for the transition time, and established the theoretical bases for generating stripping pseudopolarograms by PSA:

$$\tau = \frac{n}{2}\frac{C^0_{M^{n+}}}{C^0_{Hg^{1+}}}\frac{D_{M^{n+}}}{D_{Hg^{1+}}}t_d \qquad (14)$$

and

$$E_t = E^0 - \frac{RT}{nF}\ln\left(\frac{D\tau}{\delta l}\right) - \frac{RT}{nF}\ln(1-\phi) \qquad (15)$$

where t_d is the deposition time; τ the transition time; $C^0_{M^{n+}}$ and $C^0_{Hg^{2+}}{}^0$ the bulk concentrations of the metal and mercury ions, respectively; $D_{M^{n+}}$ (or D) and $D_{Hg^{2+}}$ the diffusion coefficients of the metal and mercury ions, respectively, in the mercury phase; l the mercury film thickness; δ the diffusion layer thickness; E_t the transient potential; $\phi = (nF/RT)(E_d - E^0)$, E_d being the reaction potential; and all other symbols have their usual meanings.

The results obtained by using conventional electrodes and fiber microelectrodes showed the latter to minimize the interferences arising from bilayer perturbations or precipitation of metal derivatives on the surface of the working electrode.

Hoyer and Kryger[19] carried out a theoretical and experimental study of the potential-time transient in PSA by using a rotating mercury-film electrode. The data obtained by digital simulation using the Cranck-Nicholson finite-difference method were quite consistent with the experimental results and were used to derive relationships between peak width and signal duration in reversible analyte systems. Severe signal overlap was found to result in distorted composite signals.

Xia et al.[20] also performed theoretical and experimental studies on film potentiometric analysis using stirred and quiet solutions of copper(II) and lead(II), and derived and validated equations descriptive of the transition time in both types of solutions:

$$\tau = K\omega_p t_p^2 C_0^* \qquad (16)$$

for quiet solutions, and

$$\tau = k^{-1}[Ox]^{-1}D_0(\omega_p/\omega_s)^{1/2}t_p C_0^* \qquad (17)$$

for stirred solutions, where τ is the transition time, C_0^* the concentration of metal analyte in solution before preelectrolysis, [Ox] the oxidant concentration at the electrode surface, k the rate constant, ω_p and ω_s the rotation speed during preelectrolysis and after the potentiostat is disengaged, t_p the preelectrolysis time, D_0 the diffusion coefficient of the metal analyte, and

$$K = 0.30D_0^{7/3}V^{-1/3}A^2k^{-2}[Ox]^{-2}V^{-2} \qquad (18)$$

A being the surface area of the electrode and V the volume of the diffusion layer.

Labar et al.[21] extended their studies on film PSA by investigating the variables that control the preconcentration and stripping steps using a rotating glassy carbon disk

electrode (rde), Pb(II) as the analyte, and Fe(III) as the oxidant. The results obtained were compared with previously reported data and, except for the influence of the rde rotation speed on each step and on the analytical parameters, experiments and theory were in close agreement. Discrepancies in the effects of the rotation speed were investigated by potentiostatic coulometry and voltammetry in regard to the preconcentration step: the effects of the rotation speed were found to arise from the physical behavior of the rde. Use of the standard-addition or internal-standard method was recommended in preference over calibration curves for analytical purposes owing to the occurrence of an activation period in the electrodeposition step.

Garai et al.[22] reported a theoretical treatment for PSA as regards anodic stripping of metals in quiet solutions involved in reversible and quasireversible electrode reactions by using mercury film electrodes. The experimental results were quite consistent with calculated data, and derivations based on various assumptions (e.g., stripping in stirred solutions, a diffusion layer of constant thickness) were compared. These authors supported the recommendation by Labar et al. as regards recording the transition time for a quiet solution, but pointed out that the reported $\delta_{Hg}/\delta_{Me} = 20$ (where δ is the diffusion layer thickness) was too high a ratio for a quiet solution, and assigned it a value of 5 to 10, depending on the rotation speed during plating. The equation derived for the transition time was

$$\tau = \frac{z_{Me}\delta_{Hg}D_R c_0^0}{z_{Hg}\delta_{Me}D_{Hg}c_{Hg}} t_{el} \qquad (19)$$

where τ is the transition time, z the number of electrons exchanged in the electrode reaction, D the diffusion coefficient, δ the diffusion layer thickness, t_{el} the preelectrolysis time, and c the concentration of metal or mercury ions in solution, which is dependent on the mercury film thickness (this is at variance with the values reported by Chau et al.[15] and proportional to the first power of the charge of the metal ion, in contrast to the peak current observed in ASV).

On the other hand, in calculating the function relating the potential and time in a PSA experiment, Garai et al. assumed the metal to distribute uniformly within the mercury film. This assumption differs from those of Hussam and Coetzee[18] and De Vries and Van Dalen,[23,24] who postulated a parabolic metal distribution in the mercury film. A uniform distribution of the metal appears to be more realistic according to Garai et al. because the literature almost unanimously demonstrates that a homogeneous metal distribution in the amalgam can be reached in a very short time. The equation

$$E = E^0 + \frac{RT}{z_{Me}F}\left[\ln\frac{2d}{(D_R\pi)^{1/2}} + \ln\left(\frac{t^{1/2}}{\tau - t}\right)\right] \qquad (20)$$

and that derived by Hussam and Coetzee show that the E-t functions have identical forms, irrespective of the assumption regarding the metal distribution in the amalgam and the stripping conditions (whether stripping is done in a stirred or quiet solution). The two equations differ by a shift in the potential of 9 or 14 mV, depending on whether the electrode process involves the exchange of one or two electrons, respectively.

Jin and Wang[10] derived and experimentally validated equations for the derivative of time with respect to potential, as well as the peak half-width for a reversible process in adsorption stripping potentiometric analysis in both stirred and unstirred solutions on the assumption of strongly adsorbed oxidized and reduced forms and obeyance of the Langmuir isotherm. The equation for an oxidant in a stirred (or unstirred) solution is of the form

$$\left(\frac{dt}{dE}\right)_p = \frac{nFt}{4RT} \qquad (21)$$

where

$$\tau = \frac{\Gamma_R t_a}{\frac{n'}{m} k D_{OX}^{2/3} v^{-1/6} \omega_0^{1/2} c_{OX}} \qquad (22)$$

for stirred solutions, and

$$\tau = \frac{\delta \Gamma_R t_a}{\frac{n'}{m} D_{OX} c_{OX}} \qquad (23)$$

for unstirred solutions, τ being the transient time; m and n′ the stoichiometric coefficients for the reaction between the reduced species adsorbed at the electrode and the oxidized species, respectively, D_{ox} (cm^2/s) the diffusion coefficient of the oxidant, v (cm^2/s) the kinematic viscosity, ϖ_0 (rad/s) the angular velocity in the bulk solution, c_{ox} (mol/cm^3) the oxidant concentration, Γ_R (mol/cm^2) the surface concentration of the adsorbed reduced species, and t_a the preconcentration time.

At the peak half-height,

$$\frac{dt}{dE} = \frac{1}{2}\left(\frac{dt}{dE}\right)_p = \frac{nF\tau}{8RT} \qquad (24)$$

so the peak half-width will be given by

$$W_{1/2} = \frac{3.52RT}{nF} \qquad (25)$$

(at 25°C, $W_{1/2}$ = 90.6/n mV).

A comparison of the equations for the peak potential, peak half-width in adsorption chronopotentiometry, and adsorption in PSA with oxidation in a stirred or unstirred solution reveals that their forms are identical. So is that for the dt/dE function, except for the sign and the definition of the transition time.

Garai et al.[25] developed and experimentally checked the theory of dPSA, based on the equation

$$\frac{dE}{dt} = \frac{\frac{RT(\tau+t)}{zF}}{2t(\tau-t)} \qquad (26)$$

as well as differential potentiometric analysis, which designates the technique based on the derivative of time with respect to potential against the potential function as the measured signal. Notwithstanding the vast application and flexibility of both techniques, no related mathematical expressions have so far been reported. The technique called "differential potentiometric analysis" by Kryger[8] does not correspond exactly to the function discussed by Garai et al. as differential potentiometric stripping analysis; however, the latter closely approximates the readout obtained by the former method, as well as multiscanning PSA as conceived by Mortensen et al.[7] and Renman et al.[4]

Zie and Huber[9] derived the equation for the transient potential-time curves in CCEPSA:

$$E_t = E^0 + \frac{RT}{nF}\ln\left(\frac{2l}{(\pi D_0)^{1/2}}\right) + \frac{RT}{nF}\ln\left(\frac{t^{1/2}}{\tau_c - t}\right) \qquad (27)$$

where l is the mercury film thickness, D_0 the diffusion coefficient of the metal ion in solution, t time, and

$$\tau_c = \frac{0.62 D_0^{2/3} v^{-1} \omega^{1/2} t_d C_{Ox}^*}{\frac{kC_{Ox}^* - I_c}{nFA}} \qquad (28)$$

the stripping time for catalytic current PSA with stirred deposition and quiescent stripping conditions, I_c being the constant cathodic current applied during the stripping step, t_d the deposition time, C_{Ox} the oxidant

concentration in the bulk solution, k the oxidation rate constant, D_0 the diffusion coefficient of dissolved metal ions, ν the kinematic viscosity, and ω the angular velocity of the solution phase, which is the same as that for conventional PSA. From Equation 27 it follows that, whether oxidation of deposited amalgam is effected by a constant oxidation flux or a "reduced" oxidant flux, the shape of the transient potential-time curves will be the same.

IV. INSTRUMENTATION IN PSA

The basic experimental set-up needed for a potentiometric stripping experiment comprises a potentiostatic circuitry, a three-electrode electrochemical cell, and an impedance recorder (Figure 10). However, the inception of novel PSA variants and attempts at improving their performance calls for some extent of automation. This has been implemented in various ways, including commercially available instruments such as the Radiometer ISS 820 Ion Scanning System or the Radiometer PSU 20 TraceLab potentiometric stripping unit, as well as customized microcomputer-controlled configurations built from electrochemical equipment typically available at laboratories (Figure 11).

Potentiometric stripping, particularly at very high stripping rates, very short plating times, or very low concentration levels of the determinants, entails recording relatively rapid potential changes. In addition to chemical and hydrodynamic conditions affecting detectability in a given determination, the time resolution of the analog strip-chart recorder is also greatly influential. Several authors have found it advantageous to use digital signal processing in this context. This can be done by using a customized dedicated microprocessor system[26] or a minicomputer with satellite process controlling measurements.[27] Most often, commercially available microcomputers are employed,[4,11,28-33] and the potential of the working electrode is sampled at frequencies from 7[29] to 26 kHz.[4] By equipping the electrochemical module

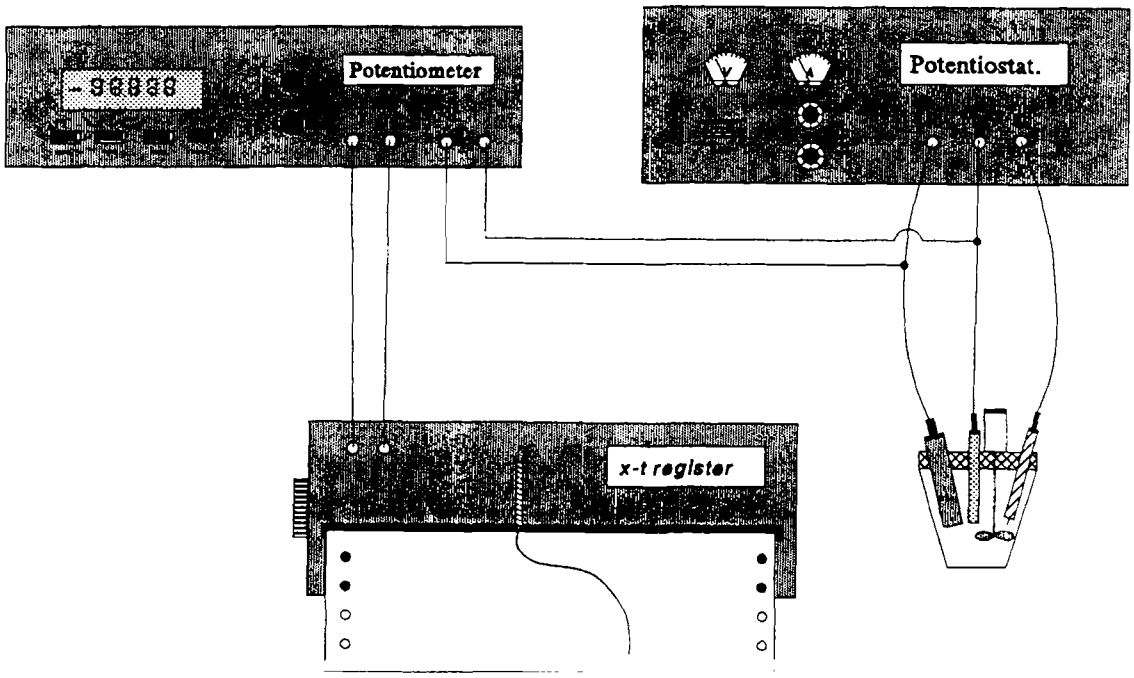

FIGURE 10. Basic instrumentation for potentiometric stripping analysis.

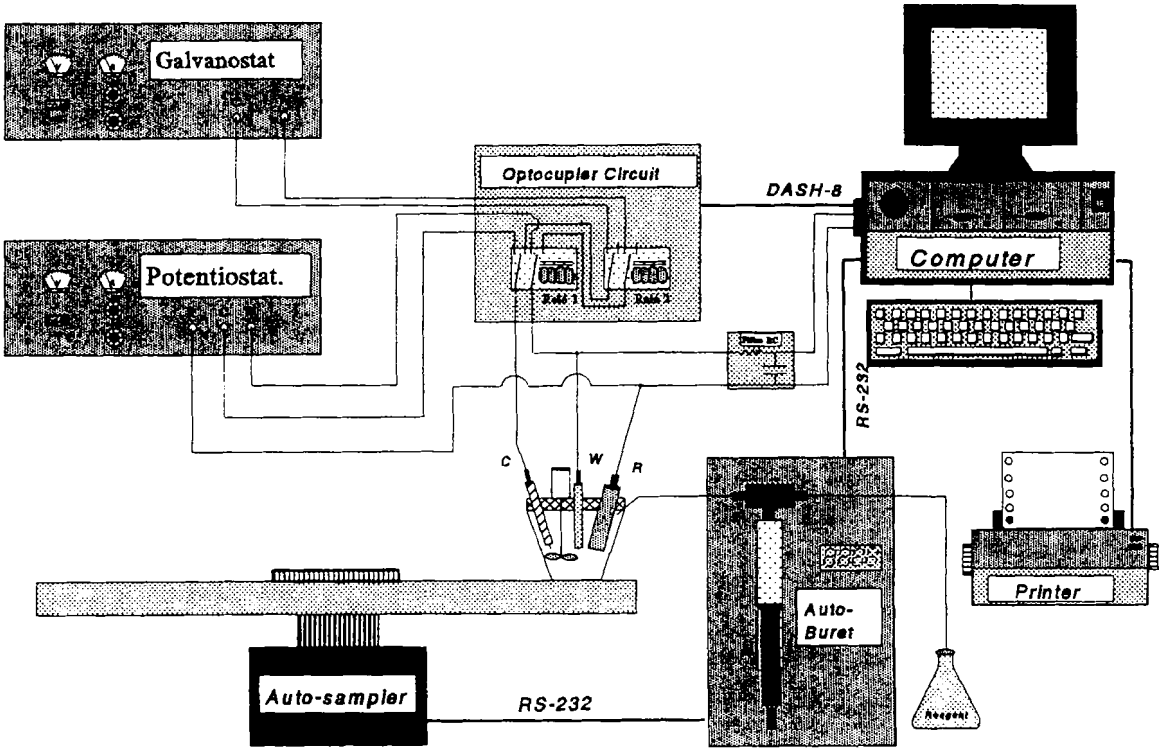

FIGURE 11. Block diagram of a computerized instrumental for PSA experiments with galvanic or chemistry stripping. (From Cladera, A.; Estela, J. M.; Cerdà, V. *J. Electroanal. Chem.* **1990,** *288,* 99–109. With permission.)

with separate memory, which is updated in hardware during the recording of the stripping step, an extremely high acquisition rate (660 kHz) was achieved with a system interfaced to an Apple IIe microcomputer.[30]

A. Electrochemical Cells and Electrodes

The earliest working electrodes used in PSA were of the dropping mercury type;[1] however, they soon proved impractical and were superseded by the rotating glassy carbon rod electrode, in which the carbon rod was coated with a mercury film, and a platinum wire was used as the counterelectrode and calomel as the reference electrode.[2] The three-electrode suite was connected to a glass or polyethylene vessel of 20 to 100 ml that allowed samples to be deaerated if desired and an oxygen-free atmosphere to be maintained by bubbling a nitrogen or argon stream (Figure 12).

The working electrode has received the greatest attention in PSA studies and applications. Although the glassy carbon rod electrode has to date been the most widely used in both analytical applications and theoretical studies, several alternative electrodes have been tested in order to improve the applicability, reproducibility, sensitivity, and selectivity of this technique (Figure 13).

For Hg(II) determination,[34] the glassy carbon rod electrode is coated with a copper film and potassium permanganate is used as the oxidant.

A copper coating over a gold film electrode has also been used for the indirect determination of chlorine-containing species.[35]

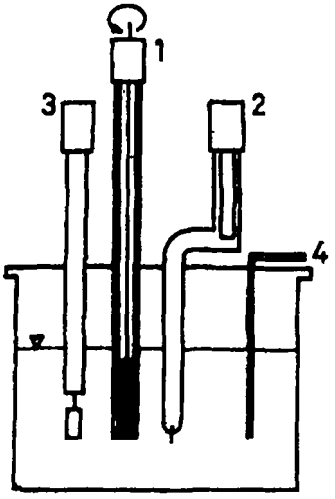

FIGURE 12. Electrochemical cell for potentiometric stripping analysis. 1, rotating film mercury glassy-carbon electrode; 2, reference electrode; 3, Pt auxiliary electrode; 4, N_2 trap.

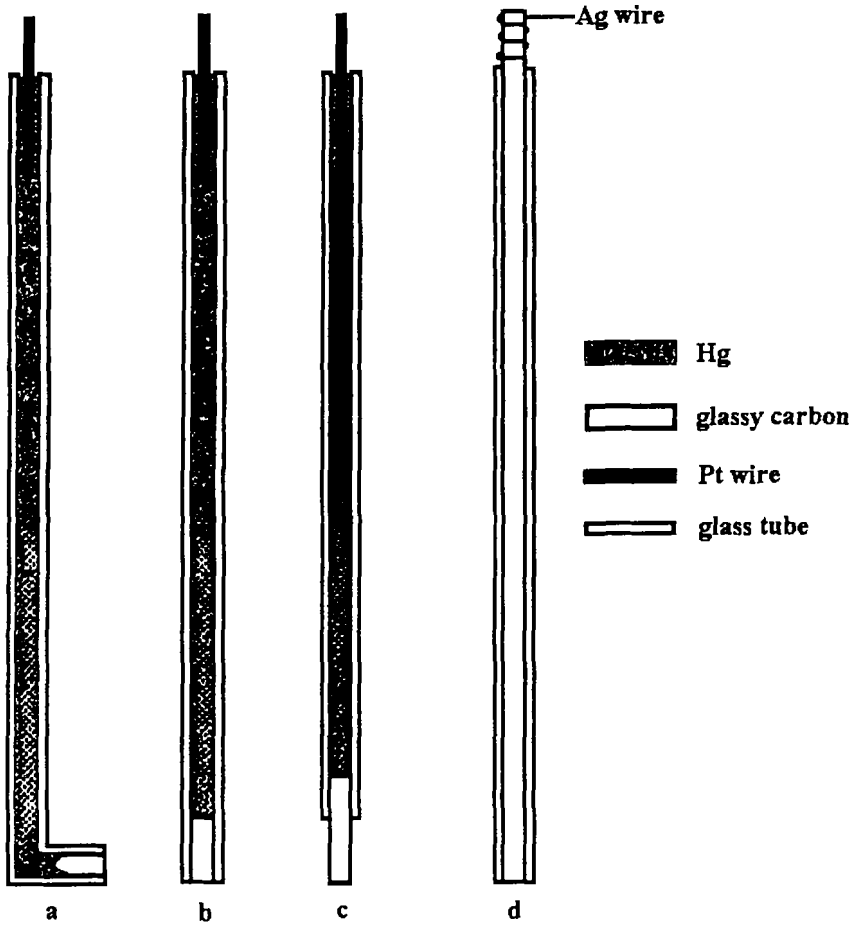

FIGURE 13. Working electrodes used for potentiometric stripping analysis. Electrodes a, b, and d have a total electrode area of 8 mm^2 and electrode c, 110 mm^2. (From Jagner, D.; Arén, K. *Anal. Chim. Acta.* **1978,** *100,* 375–388. With permission.)

In RPSA,[13] the working electrode is usually a small mercury pool that is placed in a conical cavity in the bottom of the cell when an amalgamated metal is employed as a reductant in the stripping step. If a dissolved chemical reductant is used instead, a glassy carbon or platinum electrode is fit for the purpose (e.g., in the determination of Mn(II) by use of dissolved hydroquinone as reductant and a Pt electrode because of its higher reproducibility relative to glassy carbon.

Arsenic(III) can be determined by using a gold electrode or a glassy carbon electrode coated *in situ* with gold plus arsenic during the preelectrolysis step.[36] The coating film is obtained by adding Au(III) to the sample, which also acts as the oxidant during the stripping step.

Dexiong et al.[37] used a rotating glassy carbon disk electrode with a mercury film coating for the adsorption PSA for germanium, where Alizarin Red complex is formed and adsorbed at the electrode, thereby increasing the sensitivity.

In 1984, Schulze and Frenzel[38] introduced high-modulus carbon fibers as working electrodes for PSA. They used four types of such electrodes (Figure 14): single-fiber, cut-fiber, fiber-bundle, and cut-bundle electrodes, the small surface area of which resulted in decreased background signals and hence excellent signal-to-noise ratios. Also, because of their small size, fiber electrodes (particularly the cut-fiber electrode) offer major advantages for processing small sample volumes and as detectors for flow systems.

Baranski and Quon[39] used a mercury-coated carbon fiber microelectrode as the working electrode in the microdetermination of heavy metals; they used microelectrochemical cells (Figure 15) and an amalgamated gold wire as reference electrode.

Frenzel[40] designed a microcell (Figure 16) consisting of a glassy carbon tube in-

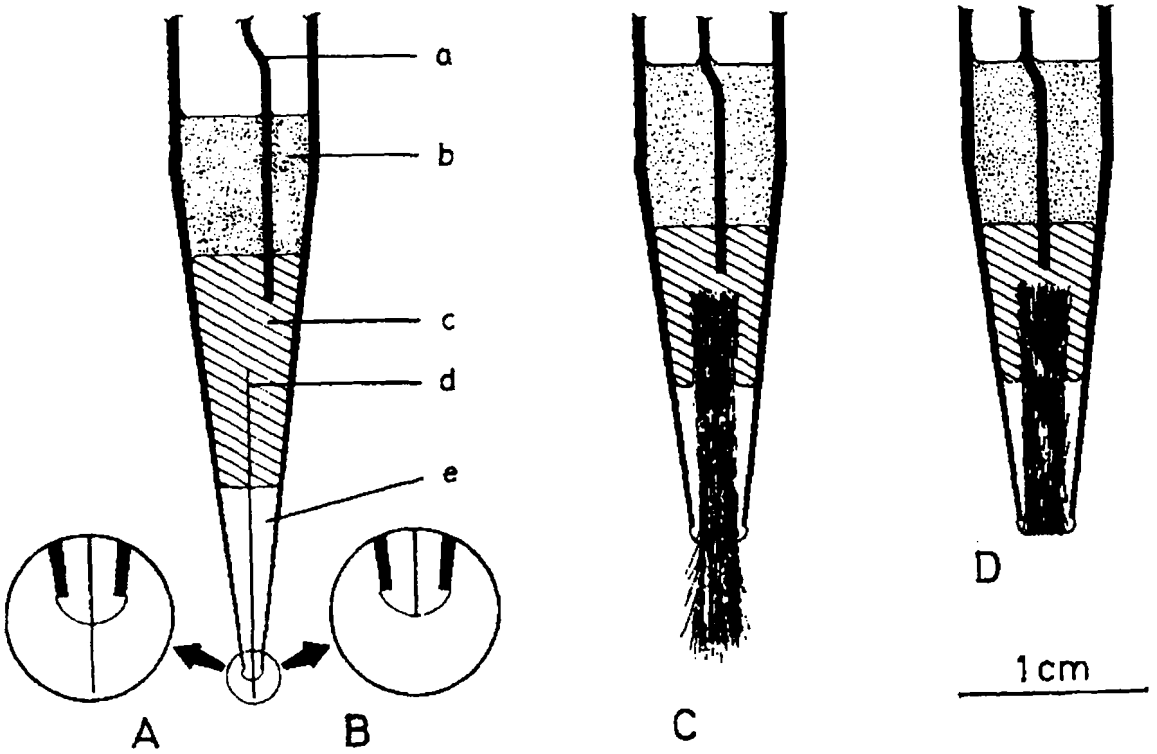

FIGURE 14. Carbon fiber electrodes. (A) single-fiber electrode; (B) cut-fiber electrode; (C) fiber bundle electrode; (D) cut-bundle electrode. (a) Silver wire; (b) epoxy resin; (c) mercury; (d) carbon fiber; (e) cyanacryl glue. (From Schulze, G.; Frenzel, W. *Anal. Chim. Acta.* **1984,** *159,* 95–103. With permission.)

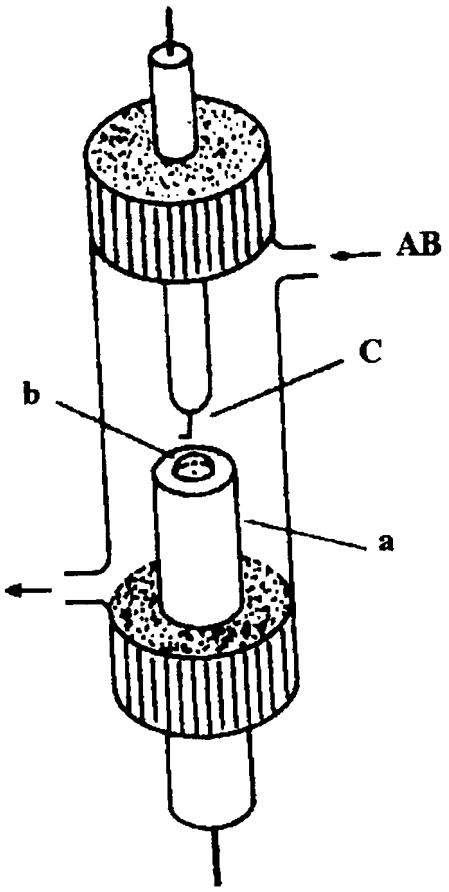

FIGURE 15. Electrochemical cell used in microanalysis. (a) Working electrode (carbon fiber sealed in polyethylene); (b), analyzed solution; (c), reference electrode (amalgamated gold wire). (From Baranski, A. S.; Quon, H. *Anal. Chem.* **1986,** *58,* 407–412. With permission.)

tended to act as an auxiliary electrode. The tube was stuck on a nipple in the center of a perspex cylinder. In this way, a small beaker-like vessel was formed with an approximate volume of 20 µl — sample volumes as low as 5 µl could be used, however. A laboratory-made Ag/saturated AgCl reference electrode was inserted upward into the perspex block and connected to the cell via a 0.1-mm bore in the center of the nipple. A diaphragm was made by plugging a small portion of quartz wool into the bore. The fiber working electrode was held by an ordinary laboratory stand and was carefully lowered into the beaker until the tip was dipped into the sample solution.

Based on the results reported by Albery and Bruckenstein,[42] who demonstrated the complete hydrodynamic equivalence of the wall-tube electrode and the rotating disk electrode, Kapauan[41] constructed a PSA cell by using a wall-tube electrode configuration with a built-in centrifugal pump (Figure 17). The reproducibility of the system was tested by using 0.4 µg/ml solutions of zinc, cadmium, and lead at a plating voltage of –1.37 V vs. Ag/AgCl that was applied for 10 s. The relative standard deviations of the measured plateau lengths in six runs were 1.1, 0.6, and 1.8% for zinc, cadmium and lead, respectively.

Alternative types of working electrode used for enhanced selectivity include chemically modified electrodes (CMEs) and physically (membrane-coated) modified electrodes. A dimethylglyoxime chemically modified graphite paste electrode was used for the determination of Ni(II).[43] The electrode was made by mixing spectroscopic-grade graphite powder, dimethylglyoxime, and DC200 silicone oil in a 1-ml polyethylene syringe. The surface of the working electrode (3 mm^2) was renewed daily by pressing out of the syringe a 1-mm layer of paste and removing it with filter paper. Electrical contact was effected by means of a silver wire inserted in the paste. The potentiometric stripping determination of Ni(II) with this graphite-paste CME involves three steps; the first and second are similar to those in conventional voltammetric stripping determinations, viz., chemisorption of Ni(II) ions on the CME surface and reduction of the preconcentrated nickel at a sufficiently negative potential. In the third step, however, nickel reduced on the electrode surface is oxidized chemically by atmospheric oxygen.

Two general types of polymer-modified electrodes (PMEs) have also been used in stripping analysis in order to improve the selectivity (by protecting the surface of the

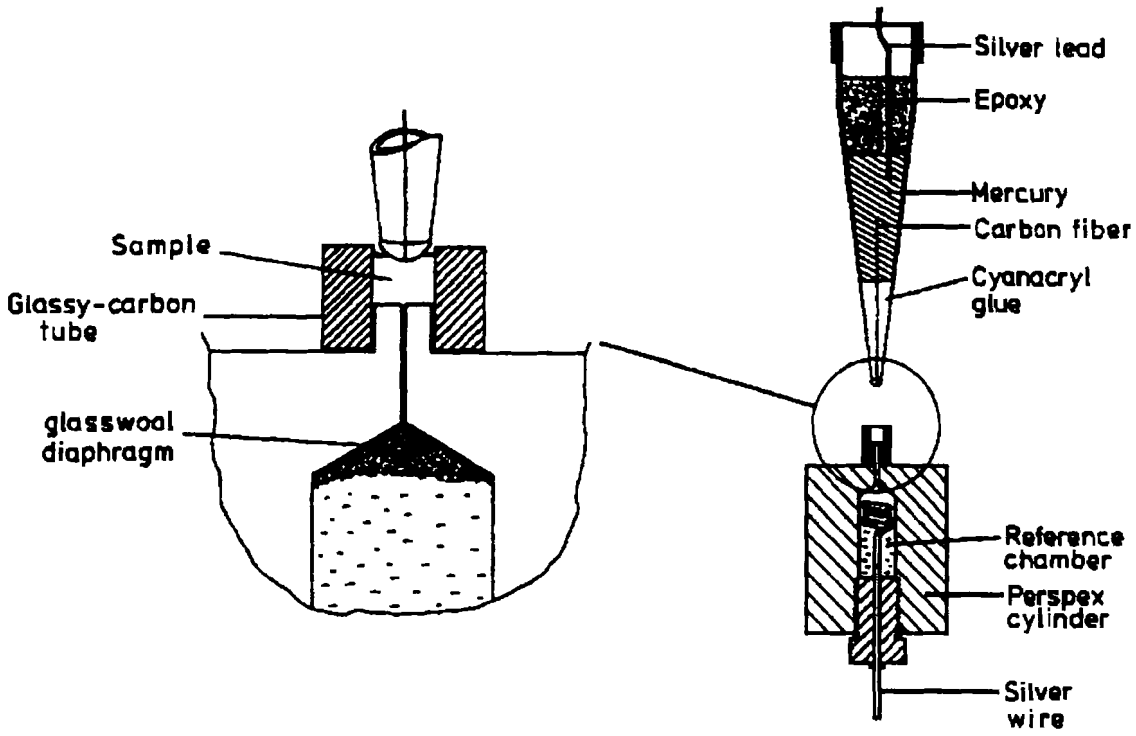

FIGURE 16. Schematic representation of a microliter-capacity cell. (From Frenzel, W. *Anal. Chim. Acta.* **1987,** *196,* 141–152. With permission.)

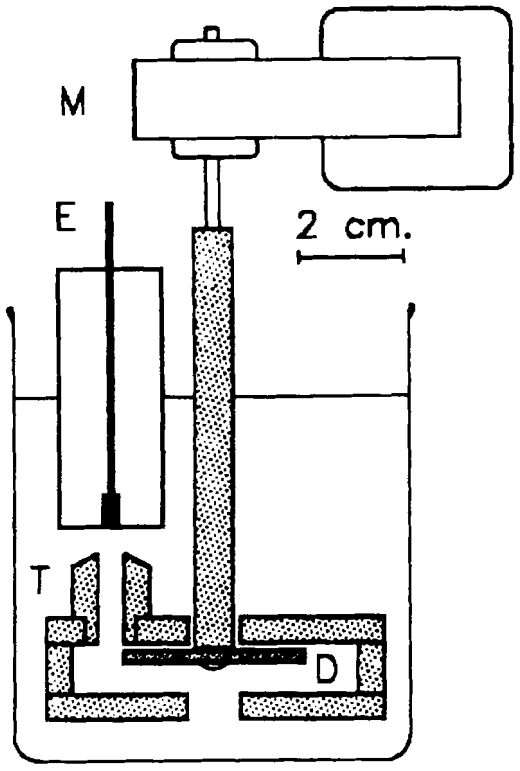

FIGURE 17. Cross section of a wall-tube PSA cell. (From Kapauan, A. F.; *Anal. Chem.* **1988,** *60,* 2161–2162. With permission.)

working electrode from adsorptive interferences): specific and nonspecific. Specific PMEs are ion-exchanging polymers (ionomers) that selectively preconcentrate the analyte within the polymer, whereas nonspecific PMEs control access to the electrode surface by acting as diffusion barriers. The perfluorosulfonate cation-exchange resin Nafion has been used as a specific PME material in both anodic stripping voltammetry (ASV) and PSA[44] for the determination of heavy metals in various environmental and clinical samples. For nonspecific PMEs, cellulose acetate dialysis membrane-modified mercury film electrodes (CM-MFEs) have been used in ASV and PSA.[3] The nonspecific cellulose acetate PME material is more advantageous in routine applications than is the specific Nafion PME material, primarily as a result of significant preconcentration by the latter. Six or more replicates per sample are required to obtain a steady signal using a Nafion-modified MFE in ASV, and consecutive samples exhibit carryover.[45] The nonspecific cellulose acetate dialysis membrane-modified MFE does not preconcentrate analyte so severely, so it requires fewer replicates per sample and minimizes carryover. The main disadvantage of using a CM-MFE arises from the presence of a relatively thick membrane at the redox surface, which results in diminished sensitivity. However, the sensitivity of a CM-MFE (1000-amu cutoff) is lower than that of an unmodified MFE by a factor of ~18 in ASV but only ~6 in PSA.

For a nonspecific polymer such as cellulose acetate, dialysis occurs across the solution/membrane-electrode interfaces. The driving force of dialysis is the concentration gradient across the membrane, where the membrane's permeability governs partitioning between it and adjacent phases. The flux J across the membrane is given by

$$J = \frac{dx}{dt} C_s = P(C_s - C_d) \qquad (29)$$

where x is the direction normal to the membrane surface, t time, P the membrane permeability, and C_s and C_d the analyte concentrations on the sample and detector side of the membrane surface, respectively (both differ from the bulk concentrations except at equilibrium.[46] The electrochemical driving force across the membrane gives rise to a steeper concentration gradient from the change in oxidation state on amalgamation (in a 1:1 stoichiometry). The use of CCSA with a dialysis membrane-modified electrode cancels an opposing gradient of divalent cations within the membrane (i.e., the analyte vs. the Hg(II) oxidant), thereby increasing the dialysis efficiency.

Wang and Tian[47] assessed the performance of screen-printed electrodes for voltammetric and potentiometric stripping measurements of trace metals with a view to their exploitation for single-use decentralized testing. Mercury-coated carbon electrodes screen-printed on a plastic strip were found to perform comparably to conventional hanging mercury drop and mercury-coated glassy carbon surfaces. Reproducible measurements of lead in 100-µl drops were thus obtained, and a detection limit of 30 ng/ml was estimated following a 10-min preconcentration. Convenient quantitation of lead in urine and drinking water was achieved in this way. A TraceLab potentiometric stripping unit (the PSU20 model from Radiometer) furnished with an ordinary Ag/AgCl electrode and a platinum wire auxiliary electrode, a SAM20 sample station, and an IBM PS/2-55X computer were used to obtain potentiograms. In addition to having a great potential for single-use decentralized clinical or environmental testing, the highly stable response of screen-printed electrodes make them especially attractive for routine, low-cost, centralized operations.

Subsequently, Wang and Tian[48] used a mercury-free disposable lead sensor based on PSA at a gold-coated, screen-printed electrode. The combination of gold-coated carbon strips and PSA was found to yield an

analytically attractive behavior in contrast to many earlier unsuccessful attempts at monitoring lead without the involvement of mercury. Changes in peak intensity and position (relative to mercury-coated strips) provide new selectivity dimensions.

V. POTENTIOMETRIC STRIPPING ANALYSIS IN FLOW SYSTEMS

The implementation of PSA in flow systems was first proposed by Anderson et al.[49] as a logical response to the inception of microcomputers, the high data-acquisition capabilities of which allowed the preelectrolysis time to be substantially shortened; as a result, throughput was after that determined by how expeditiously sample changeover and electrode cleaning were done. This limitation could obviously be overcome by using a flow system, with the added advantage that the stripping step need not involve the sample — in contrast to batch operation — so use of a suitable stripping solution (and a matrix-exchange technique) was bound to result in enhanced sensitivity and selectivity in PSA, irrespective of the composition of the sample concerned.

The theoretical foundation of PSA in flow cells was established by Anderson et al.[49] from equations previously derived for M_iCl^+, M_iCl_2, . . . , and D_{Mi} by Hanekamp and Niewerk[50] for diffusion-controlled PSA. The amount of $M_i(n)$ reduced and simultaneously amalgamated, $M_i(Hg)$, by potentiostatic deposition on a mercury-coated glassy carbon electrode in a thin-layer cell is given by:

$$\sum_{i=1}^{m} M_i(Hg) = \int_{t=0}^{t_{dep}} \sum_{i=1}^{m} \left([M_i(n)] D_{M_i}^{2/3} \right) \gamma \nu^{1/3} \omega \left(u_{dep} l \nu^{-1} \right)^{\beta} dt \quad (30)$$

where t_{dep} (s) is the time of potentiostatic deposition, $M_i(n)$ the molar concentrations of reducible $M_i(n)$ species (e.g., M_iCl^+, M_iCl_2, . . .), D_{Mi} (cm^2/s) the diffusion constants for such species, ω (cm) the cell spacer width, ν (cm^2/s) the kinematic viscosity, l (cm) the electrode length, u_{dep} (cm/s) the mean linear flow during potentiostatic deposition, and γ and β two numerical constants.

The amount of amalgamated metal that is reoxidized (stripped), in millimoles, over a given interval $t_2 - t_1$ (s) is given by:

$$mM_i(Hg)_{stripped} = \int_{t_1}^{t_2} \sum_{k=1}^{j} \left(n m_k^{-1} [A_k(ox)] D_{A_k(ox)}^{2/3} \right) \gamma \nu^{1/3} \omega \left(u_{strip} l \nu^{-1} \right)^{\beta} dt \quad (31)$$

where $[A_k(ox)]$ is the molar concentration of one of the j different oxidants present in the stripping solution and capable of diffusion-controlled oxidation of $M_i(Hg)$ according to the reaction

$$M_i(Hg) + n m_k^{-1} A_k(ox) \rightarrow M_i(n) + n m_k^{-1} A_k(red) \quad (32)$$

and u_{strip} is the mean linear velocity during stripping.

If t_1 and t_2 are used to designate the beginning and end, respectively, of $M_i(Hg)$ stripping, the potentiometric stripping signal for M_i at $t_{Mi,strip} = t_2 - t_1$ can be represented by

$$t_{M_{i,strip}} = t_{dep} [M_i(n)] D_{M_i}^{2/3} \left(u_{dep} u_{strip}^{-1} \right)^{\beta} \sum_{k=1}^{j} \left[n m_k^{-1} A_k(ox) D_{A_{k(ox)}}^{2/3} \right]^{-1} \quad (33)$$

provided the kinematic viscosity is the same in the sample as in the stripping solution. From Equation 33 it follows that the potentiometric stripping signal for $M_i(n)$ will be independent of the overall electrode surface area.

Because in most potentiometric experiments the concentrations of the major sample matrix components (e.g., H^+ and Cl^-) are kept constant and the composition of the stripping solution is the same from one analysis to the next, Equation 33 can be rewritten as

$$t_{M_{i,strip}} \propto t_{dep}[M(n)]\left(u_{dep}u_{strip}^{-1}\right)^{\beta} \quad (34)$$

which is the fundamental equation for quantitative PSA in flow cells. Based on previous findings of Levich,[51] Hanekamp and Van Nieuwerk[50] calculated $\beta = 0.5$ for a thin-layer cell as opposed to the experimental value of 0.3 obtained by Swartzfager.[52]

The potential of the working electrode, E (V), during the stripping of $M_i(Hg)$ is given by

$$E = E^0 + RT\ln(10)n^{-1}F^{-1}\log\left[\left(M_i^{n+}\right)\left(M_i(Hg)\right)\right]^{-1} \quad (35)$$

where E^0 is equivalent to the half-wave potential in polarography and (M_i^{n+}) is the steady-state activity of M_i^{n+} accumulated at the electrode surface during stripping. From Equation 35 it follows that the stripping potential is independent of the mercury film thickness. In PSA, however, the glassy carbon working electrode is usually precoated with a film of mercury, so the relative increase in film thickness during consecutive analyses can be neglected. A side-reaction coefficient, $\alpha = [M(N)]/[M^{n+}]$, due to rapid complexation reactions at the electrode surface with different ligands thus needs to be introduced. If L is used to designate the predominant complexing agent at the electrode surface and the free concentration of L is changed from $[L]_I$ to $[L]_{II}$ in two consecutive experiments, the stripping potential shift for M_i^{n+}, ΔE (V), will be

$$\Delta E = RTn^{-1}F^{-1}\ln(10)\left(\log\alpha_{[L]=[L]_t} - \log\alpha_{[L]=[L]_m}\right) \quad (36)$$

provided complexation is not the rate-determining step in the combined oxidation-complexation reaction.

PSA as a detection technique has been used primarily in two types of flow systems: continuous-flow (CF) and flow-injection (FI) systems. Both CFSPSA and FIPSA systems are highly automated and differ in the fact that the sample is continuously driven to the detection cell during the preelectrolysis step in the former, whereas a sample volume is injected into a carrier stream that leads it to the detector (where preelectrolysis is conducted) in the latter.

CFSPSA configurations typically consist of a flow-cell accommodating a three-electrode system, in addition to a microcomputer-controlled, six-step PTFE inlet valve for sample or reagent inlets and a propulsion system that can be a peristaltic pump or a water-column suction unit via which the flow rate can be regulated. The remaining elements are those typical of conventional PSA and include a potentiostat (or, occasionally, a galvanostat) and an x-t recorder with a high-impedance input or, more commonly, a microcomputer for data acquisition and processing. The computer can also be used to actuate the six-way valve, engaged and disengage the potentiostat (galvanostat), control a sampler, and enact a series of predetermined steps. In some instrumental setups, several of these operations are performed by commercially available dedicated instruments (e.g., the Ion Scanning System ISS820 from Radiometer).

The first step in a CFSPSA application involves conditioning the working electrode. For example, a mercury film electrode can be conditioned prior to insertion into the flow cell or *in situ* (by having the valve circulate the mercury solution through the cell and applying a potential program to ensure deposition of the film). Then, the sample is circulated through the cell by switching the valve and the potentiostat is simultaneously engaged at the desired elec-

trodeposition potential and flow rate over a preset interval. Subsequently, the stripping step can be carried out by disengaging the potentiostat and either using a chemical oxidant previously added to the sample or passing an electric current. Alternatively, stripping can be accomplished by changing the matrix; for this purpose, the valve is switched before the potentiostat is disconnected in order to circulate a suitable stripping solution containing an oxidant or pass an electric current. After the sample channel is flushed, the cycle can be repeated by inserting a fresh sample.

The literature abounds with reported applications of CFSPSA systems. Anderson et al.[49] used a thin-layer cell (Figure 18) accommodating a mercury-coated glassy

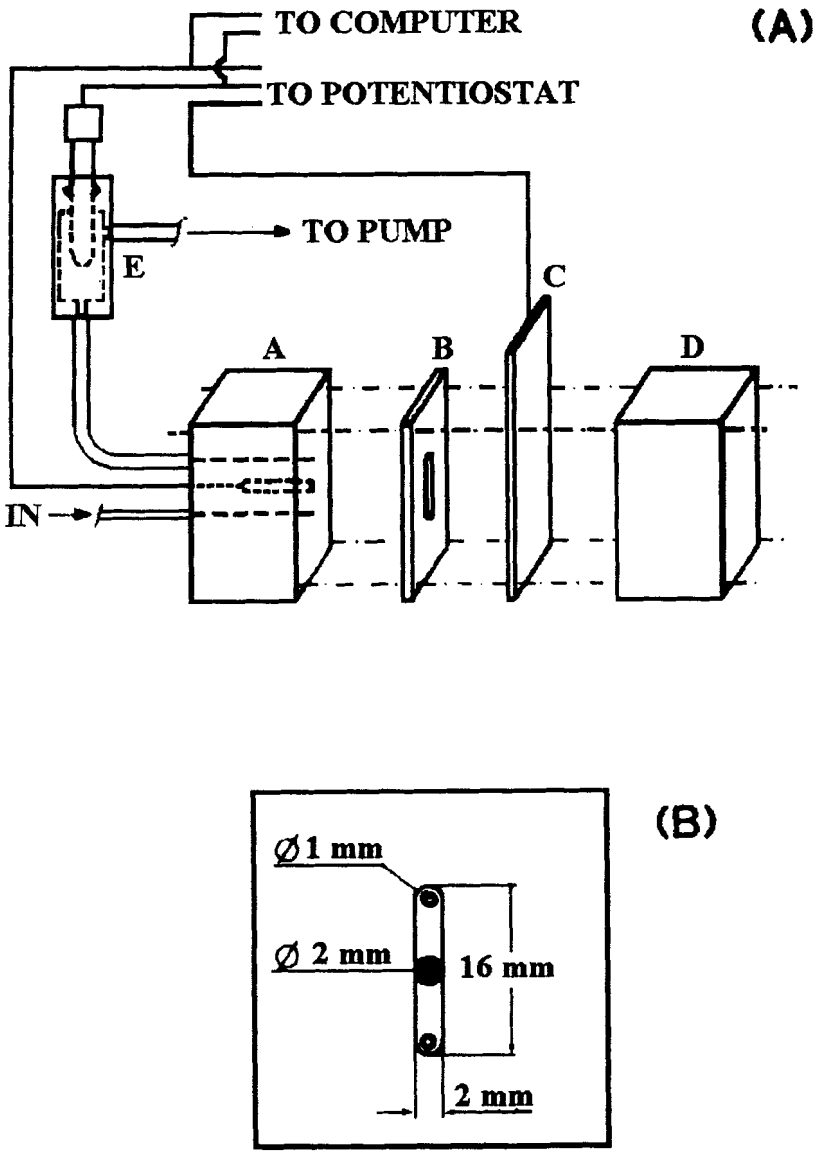

FIGURE 18. (A) Flow cell. A, PTFE block with glassy carbon electrode and sample inlet/outlet; B, PTFE cell spacer; C, Pt counterelectrode; D, PTFE block; E, reference electrode compartment. (B) Details of cell spacer, glassy carbon electrode, and sample inlet/outlet. (From Anderson, L.; Jagner, D.; Josefson, M. *Anal. Chem.* **1982,** *54,* 1371–1376. With permission.)

carbon working electrode, and matrix-exchange stripping, for the selective determination of Tl(I) in the presence of a 10^4-fold excess of Cd(II), provided the stripping solution contained at least 1 *M* ammonia. They employed the flow system (Figure 19) to determine Pb(II) in wines by using a matrix-modifying solution containing 1 *M* $CaCl_2$, 0.1 *M* HCl, and 0.25 n*M* Hg(II) in 40% ethanol.

Later, Jagner et al.[53] employed CFSPSA systems for the determination of mercury(II) in various samples of clinical (urine) and environmental interest (sediments), as well as digests from biological materials (orchard leaves and fish muscle), by use of a gold working electrode. The preelectrolysis step was carried out in a sample previously conditioned with ammonia and iodide, while stripping was done in an acidified bromide solution containing Cr(VI). By using mercury standard solutions, a detection limit of 2 n*M* was achieved after a 90-s preelectrolysis, the dynamic range encompassing nearly 3 decades. Copper(II) and silver(I) were found to interfere in a 1000- and fivefold excess, respectively, over mercury(II).

Mannino[54] used a CFSPSA system similar to one previously employed by Anderson et al.[49] in order to determine the optimal conditions for the separation and determination of lead and tin in fruit juices and soft drinks. Preelectrolysis was carried out in a strongly acidic medium using a coated glassy carbon working electrode, while stripping was done in a deaerated ammonium nitrate solution at pH 4.6. By using the stopped-flow operational mode during stripping, lead and tin could be determined at concentrations as low as 0.1 ppb.

Eskilsson and Turner[55] used CFSA (Figure 20) with PSA detection (Figure 21) for the determination of manganese(II) over the concentration range 2 n*M* to 30 μ*M* in natural waters, as well as total manganese, following pretreatment with hydroxylamine.

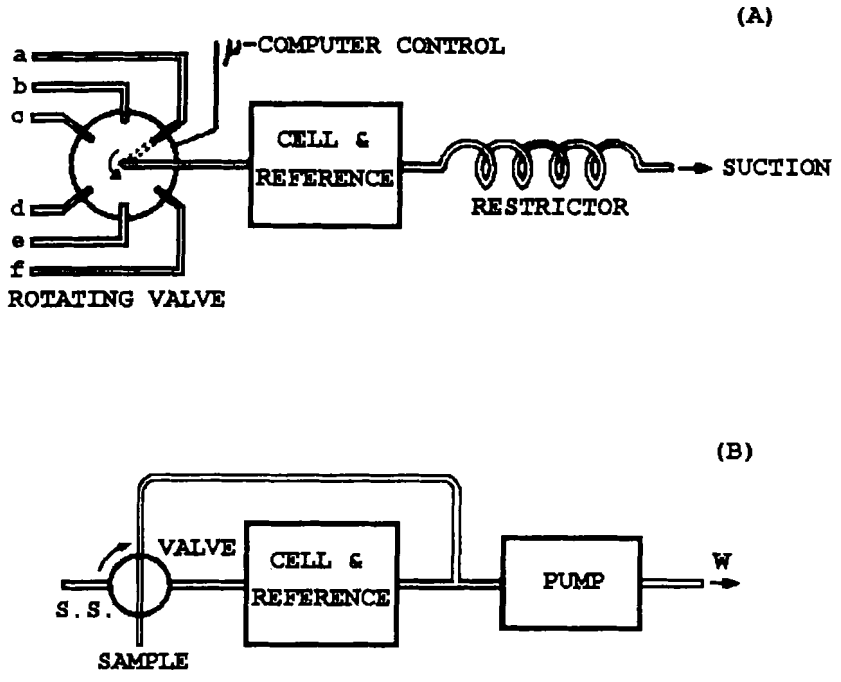

FIGURE 19. Flow system designs. (A) Continuous flow; (B) flow injection. (From Anderson, L.; Jagner, D.; Josefson, M. *Anal. Chem.* **1982,** *54,* 1371–1376. With permission.)

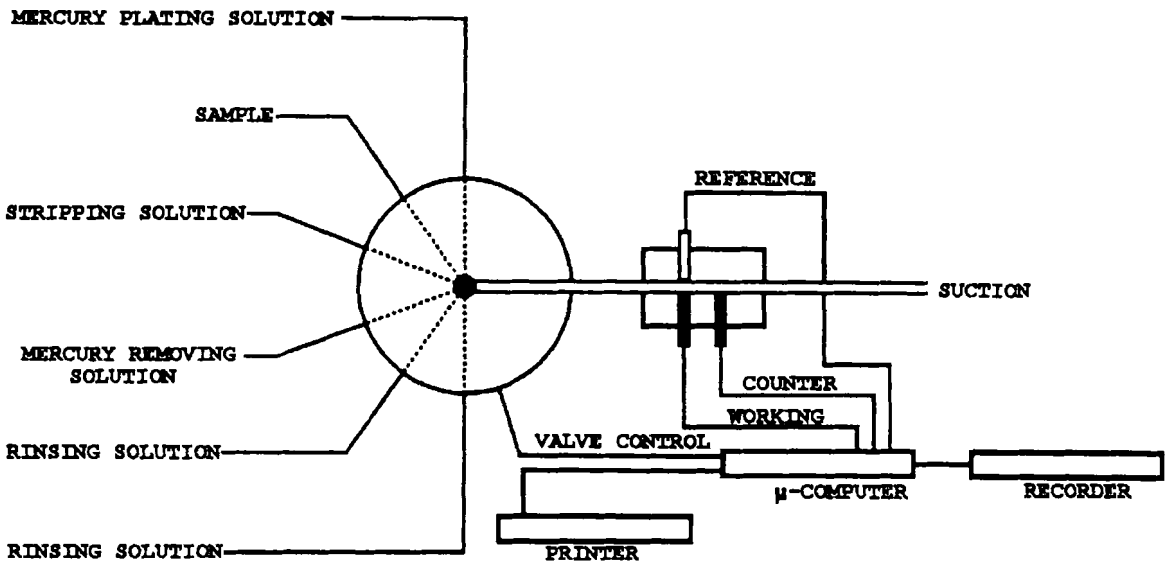

FIGURE 20. Block diagram of a PSA flow system. (From Eskilsson, H.; Turner, D. R. *Anal. Chim. Acta.* **1984,** *161,* 293–302. With permission.)

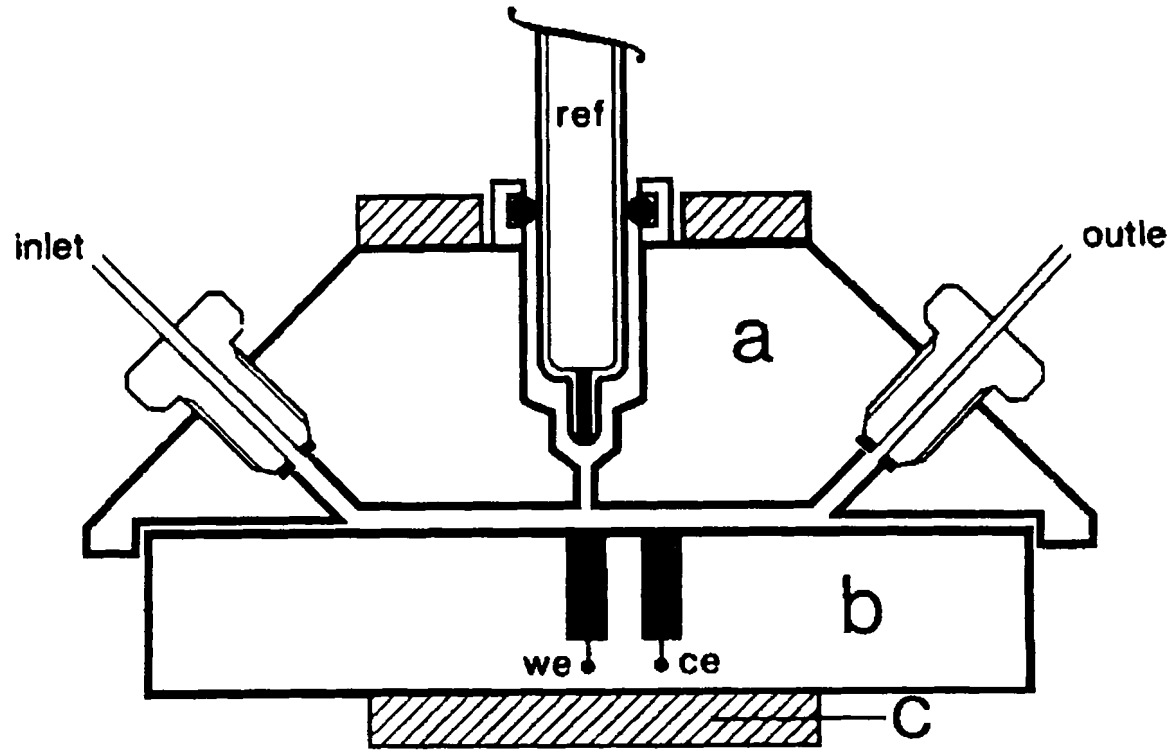

FIGURE 21. PSA flow cell. (a) Perspex block with reference electrode compartment and 1-mm flow channel; (b) teflon block containing glassy carbon working (we) and counter (ce) electrodes; (c) clamp to hold cell together. (From Eskilsson, H.; Turner, D. R. *Anal. Chim. Acta.* **1984,** *161,* 293–302. With permission.)

The experimental procedure involved removal, chemical clean-up, and subsequent regeneration of the mercury film formed over the glassy carbon working electrode after each measurement, as well as using a $CaBr_2$-saturated solution for stripping. In this way, the main problem posed by the CFSPSA determination of manganese — too rapid stripping rates arising from an incompletely irreversible reoxidation of Mn(II)-amalgamated manganese and resulting in broad, ill-defined peaks — was circumvented. The rate of chemical oxidation during stripping is a crucial parameter that is controlled by the concentration of oxidant in the stripping solution and its rate of transport to the electrode (the flow rate or rotation speed). The two parameters are adjusted in such a way as to ensure a low stripping rate for both batch and flow measurements. The oxidant concentration can be lowered for flow measurements by using saturated $CaBr_2$ as the stripping solution. This approach is necessitated by the difficulty involved in transporting a deoxygenated solution through flexible tubing, which is highly permeable to oxygen — the problem does not emerge if oxygen is insoluble in the solution used, as is the case with the calcium bromide solution. The oxidant in the stripping solution is assumed to be residual oxygen. On the other hand, interferences arising from manganese-copper interactions in the mercury electrode can be suppressed by adding zinc or gallium, depending on the concentration of interfering copper.

Dyrssen et al.[56] studied the effect of using concentrated solutions of salts on the stripping time in computerized flow PSA. They demonstrated that, for 1:1 salts, the effect was mainly due to salting out of the oxygen, while for 1:2 salts, the effect was mainly due to salting out of the oxygen, while for 1:2 salts, the effect was due to both salting out and an increased viscosity of oxygen (η) in the salt solution. They also showed the stripping time to be strongly correlated with the η/S ratio, where S denotes the solubility of oxygen in the salt solution.

Almestrand et al.[57] determined cadmium, lead, and copper in milk and milk powder with minimal pretreatment by using a highly automated CFSPSA system that enabled control of the pump rate, electrolysis time and potential, and opening and closing of valve inlets, in addition to digital evaluation of stripping times. Samples were diluted fivefold with Suprapur hydrochloric acid and electrolyzed for 0.5 to 4 min prior to stripping (also in Suprapur HCl). The analytical results were consistent with the certified values for three milk powder reference samples. The detection limits for cadmium, lead, and copper in milk samples achieved after 4-, 1-, and 0.5-min preelectrolysis were 0.8, 4, and 8 μg/l, respectively.

Renman et al.[4] developed a computer-assisted system for PSA measurements in a CFS configuration using a chemical oxidant or a constant electric current for stripping, and a new cell design (Figure 22). The thin-layer cell was designed for accommodating Teflon-embedded glassy carbon electrodes in a spring-regulated holder, allowed ready fastening, and exhibited leak-free behavior. Subsequently, the design was used for the determination of molybdenum(VI) in sea water[58] by potentiostatic adsorption of the 8-quinolinol complex of the metal onto a mercury-film electrode and subsequent reduction of the complex by constant-current stripping in 5 *M* $CaCl_2$.

Huiliang et al.[59] used carbon fiber electrodes in flow potentiometric and constant-current stripping analysis applications. The signal-to-noise ratio was approximately 1.6 times higher for an 8- to 10-μm carbon fiber relative to the glassy carbon disk electrode. The use of fiber electrodes for the determination of metal ion concentrations by a current-measuring technique such as amperometry or voltammetry often poses instrument problems arising from the very low currents to be monitored. This problem does not apply to PSA because the technique's

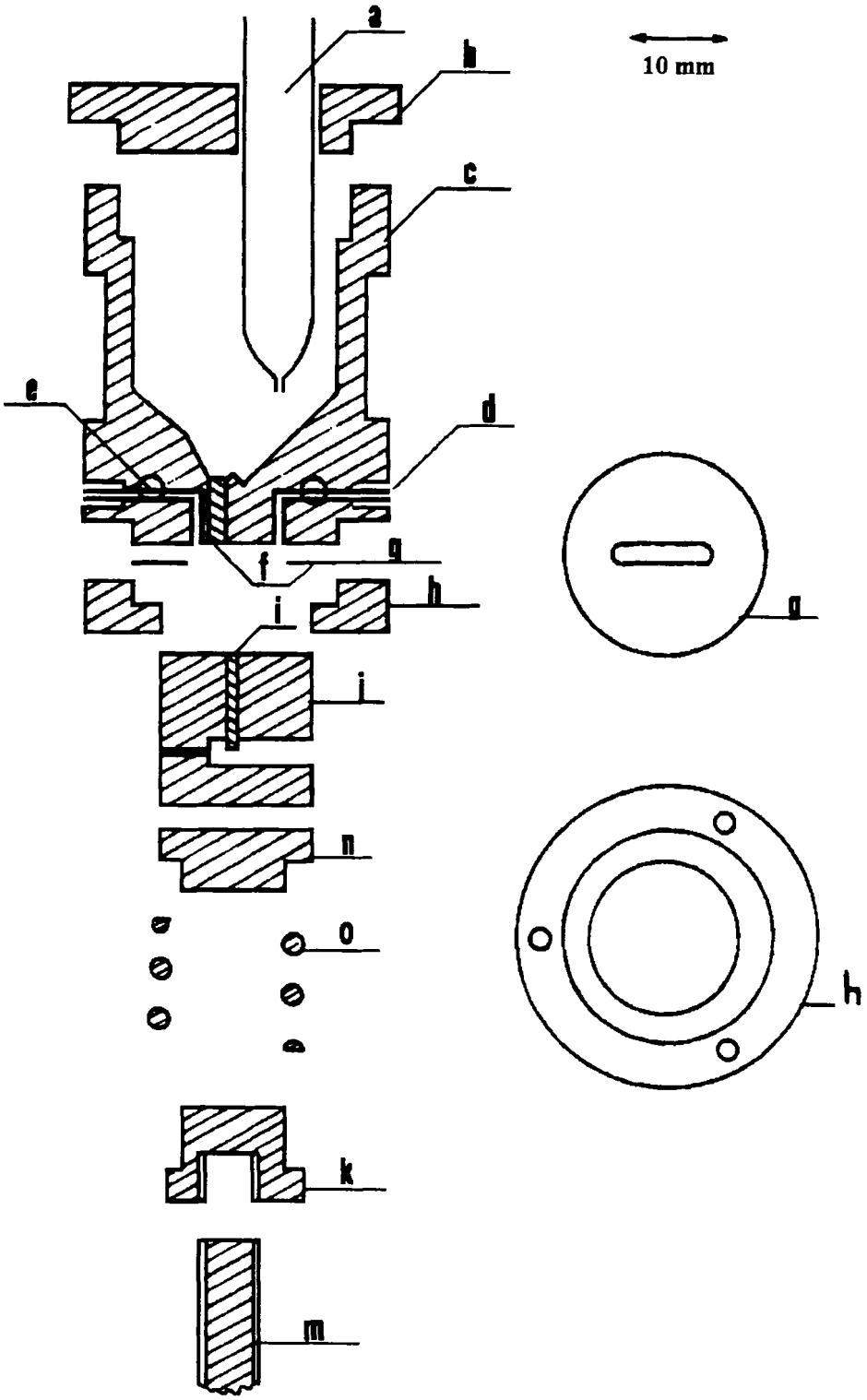

FIGURE 22. Flow cell assembly. (a) Calomel reference; (b) reference compartment lid; (c) reference compartment; (d, e) platinum tube flow inlet and outlet; (f) ceramic plug; (g) polyethylene spacer; (h) spacer holder; (i) glassy carbon rod; (j) teflon body; (k, m) titanium holder; (o) spring; (n) holder top. (From Renman, L.; Jagner, D.; Berglund, R. *Anal. Chim. Acta.* **1986,** *188,* 137–150. With permission.)

performance is independent of the surface area of the working electrode. For this reason, fiber electrodes were recognized as suitable for use in PSA.[38,39,60] In contrast to the potentiometric stripping signal, the magnitude of the constant-current stripping signal is dependent on the surface area of the working electrode. Consequently, fiber electrodes can be assumed to be inferior to glassy carbon disk electrodes and other types of macroelectrodes used in CCSA. However, based on the experimental results obtained by using fiber electrodes with chemical or electrical stripping in addition (usually) to a matrix-exchange technique, in the determination of lead in urine,[61] cadmium and lead in whole blood[62] with carbon fiber electrodes, arsenic(V) in sea water with a gold-coated, platinum-fiber electrode,[63] silver(I) with a platinum-fiber electrode,[64] gold(III) with carbon and platinum fiber electrodes,[66] and Zn(II), Cd(II), and Pb(II)[44] or organic compounds such as erythromycin[67] in urine by use of modified Nafion carbon fibers and mercury-coated fiber electrodes, they are as good as or even better than other types of electrodes typically used in PSA.

In flow injection PSA (FIPSA) (Figure 23), fixed-size aliquots of the unknown are inserted at preset times into a carrier flowing stream by using an autosampler operating in conjunction with a sample-loop/chromatographic switching valve combination. With proper consideration of variables such as the tubing diameter and flow rate, the sample plug is carried along the system with very limited dispersion into the carrier on either side. The injected plug can be passed by an electrode where plating of the metal ions to metal occurs. After the plug has passed by this point, potentiometric stripping can occur in the carrier environment. The working glassy carbon electrode is usually plated with mercury *in situ* by adding mercury ion to the sample, thus leading to the formation of analyte amalgam during the plating process.

The theoretical foundation of the FIPSA technique, as established by Hu et al.,[68] is as follows: the limiting current i_l at a flow-through planar electrode was formulated by Levich[51] as

$$i_l = nkFC_b v_f^x \qquad (37)$$

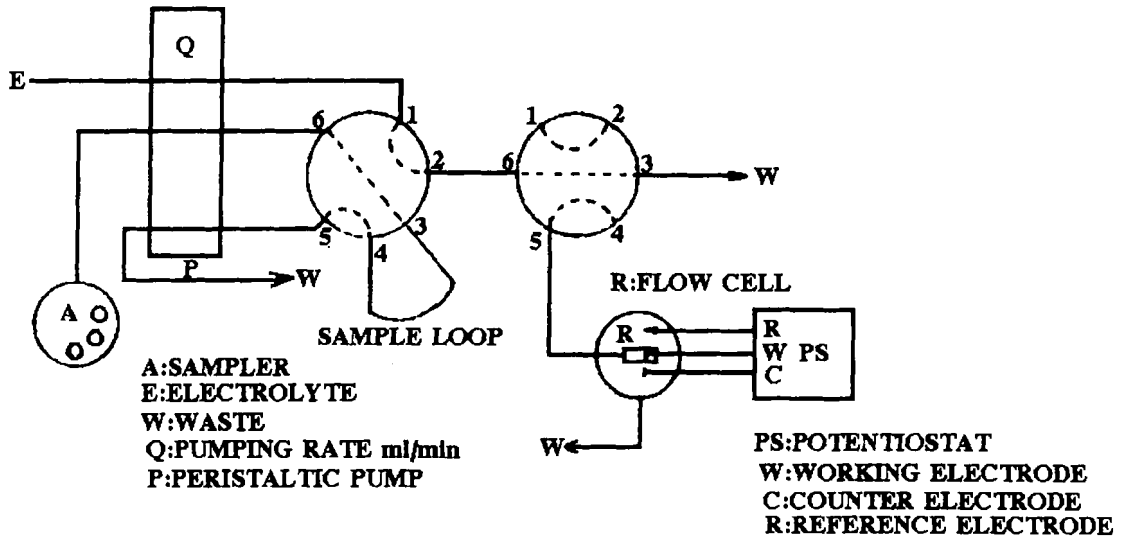

FIGURE 23. Block diagram, FIA/PSA instrument. (From Hu, A.; Dessy, R. E.; Granéli, A. *Anal. Chem.* **1983,** *55,* 320–328. With permission.)

where n is the number of electrons involved in the process; F the Faraday constant; C_b the bulk concentration of the electroactive species; v_f the flow velocity; k a complex function of the diffusion coefficient, the kinematic viscosity of the fluid, and the electrode geometry; and x a constant calculated theoretically to be 1/3 for the tubular electrode and 1/2 for the planar electrode.

For a given set of experimental conditions, k is constant, so

$$i = Kv_f^x \tag{38}$$

where $K = nkFC_b$.

The amount of analyte Q deposited in a glassy carbon electrode over the electrolysis period can be calculated from

$$Q = i_l t_{elec} \tag{39}$$

where t_{elec} is the electrolysis time.

In flow injection analysis, the sample is injected into the flow stream as a plug. Therefore, the time during which it is exposed to the electrode surface determines the effective plating time, which can thus be defined as

$$t_{elec} = \frac{V_s}{v_f} \tag{40}$$

where V_s is the sample volume and v_f the flow velocity.

Appropriate combinations of Equations 38 to 40 yield

$$Q = i_l t_{elec} = i_l \frac{V_s}{v_f} \tag{41}$$

$$Q = KV_s v_f^{x-1} \tag{42}$$

According to Equation 42, the amount of analyte plated out is inversely proportional to the flow rate.

If the limiting current can be measured at various flow rates, a plot of log (v_f) vs. log (i_l) will give a straight line of slope x. Likewise, if the amount of analyte deposited can be experimentally determined, a plot of Q vs. log (v_f) will also give a straight line of slope x – 1.

Buffle et al.[69] related the rate of oxidation to the oxidant concentration by

$$\frac{dN}{dt} = \frac{AD(C_b - C_0)}{H} \tag{43}$$

where dN/dt is the rate of oxidation, A the electrode surface area, D the diffusion coefficient, H the diffusion layer thickness, C_b the bulk oxidant concentration, and C_0 the oxidant concentration at the electrode surface.

If the oxidation process is diffusion-controlled and the bulk oxidant concentration is much larger than that at the electrode surface, Equation 43 simplifies to

$$\frac{dN}{dt} = \frac{ADC_b}{H} \tag{44}$$

Consequently, the rate dN/dt remains constant provided the oxidant concentration C_b remains unchanged. Bruckenstein and colleagues[70,71] and Jagner and colleagues.[1,2,26,72,73] investigated the matter and found the simplification to be warranted. The following relationship was found to exist between Q (the amount of analyte deposited) and t_{strip} (the time need for the amalgamated metal to be oxidized):

$$Q = \frac{ADC_b t_{strip}}{H} \tag{45}$$

Therefore, the time required for stripping a metal from the electrode surface can be used to quantify the concentration of the metal in question. Because

$$\frac{KV_s v_f^{x-1}}{nF} = \frac{ADC_b t_{strip}}{H} \tag{46}$$

a plot of log (t_{strip}) vs. log (v_f) will also give a straight line of slope x – 1.

Research into FIPSA systems has been concerned primarily with the design of highly automated systems, the performance of electrochemical flow cells, and procedures for increasing the selectivity (by use of the matrix-exchange technique during stripping) and sample throughput.

Hue et al.[74] proposed an FIPSA system for the automatic determination of copper, cadmium, and lead in ground water and evaluated the performance of the matrix-exchange technique for the separation of close oxidation peaks. Heavy metals commonly found in ground water, such as lead, thallium, cadmium, bismuth, and tin, were assayed in order to explore the scope and limitations of the method. Data generated during the stripping step were digitized and acquired at a high speed by a minicomputer equipped with a satellite processor, and the digital numbers obtained for each time interval were mapped into a data file, thereby increasing the memory cell's content. Each memory cell represents a channel of a multichannel analyzer. This provides the first derivative of the stepped potential scan, yielding "peak"-type data in a direct fashion. The number of counts accumulated in the memory-mapped multichannel analyzer depends on the oxidation rate of the analyte as well as the data acquisition rate of the analog-to-digital converter used. The recorded number of counts on a channel (or cell) is proportional to the data acquisition rate and resolution of the converter (in volts per channel). It is inversely proportional to the oxidation rate, that is, the slope of the potential-time curve (in volts per second). This linear dependence of the observed signal on the data acquisition rate will have a unique slope that is characteristic of the oxidation rate at a given point on the potential time curve. Metals with different oxidation rates should exhibit a different dependence of the signal magnitude on the data acquisition rate. The relative magnitude of the signal-to-baseline ratio remains constant regardless of the data acquisition rate used. However, the absolute magnitude of the signal-to-baseline difference does increase as the data acquisition rate is raised. In other words, the minimum quantity the technique can detect can be reduced by using a high data-acquisition rate. The best analogy is the improvement in counting statistics in radiochemistry that results from an increased observation period.

Schulze et al.[75] investigated the use of the matrix-exchange technique in FIPSA. For this purpose, they measured the stripping potentials of cadmium, lead, thallium, and tin in various supporting electrolytes. The data obtained were used to optimize the composition of the carrier solution for the simultaneous determination of mixtures of these elements. Complexing agents such as citrate, tartrate, and ammonia led to a dramatic potential shift for bivalent ions, thus removing hindrances on the simultaneous determination. Among the nearly 40 different supporting electrolytes tested, NH_3/KOH was found to be so good that the four elements (Cd, Tl, Pb, and Sn) could be determined simultaneously even at concentrations differing by as much as one order of magnitude.

Frenzel and Bratter[76] proposed a FIPSA system featuring extremely short residence times (less than 1 s) and a proportionally high throughput (up to 200 samples per hour) (Figure 24). Up to four elements could be determined simultaneously at concentrations from a few micrograms per liter to several hundredths. On-line sample manipulation (dilution and matrix modification) was possible by using one- and two-channel flow systems. The utility of FIPSA was evaluated by comparing the response, sensitivity, and several practical aspects of four different flow-through cells: a Metrohm EA 1096 wall-jet detector, a laboratory-made wall-jet cell, a thin-layer cell, and an open thin-layer cell. The ensuing method was used successfully for the fast sequential quantitation of zinc, lead, and copper in tap water, and the direct determination of lead and cadmium in acid digests from biological samples with no pre-

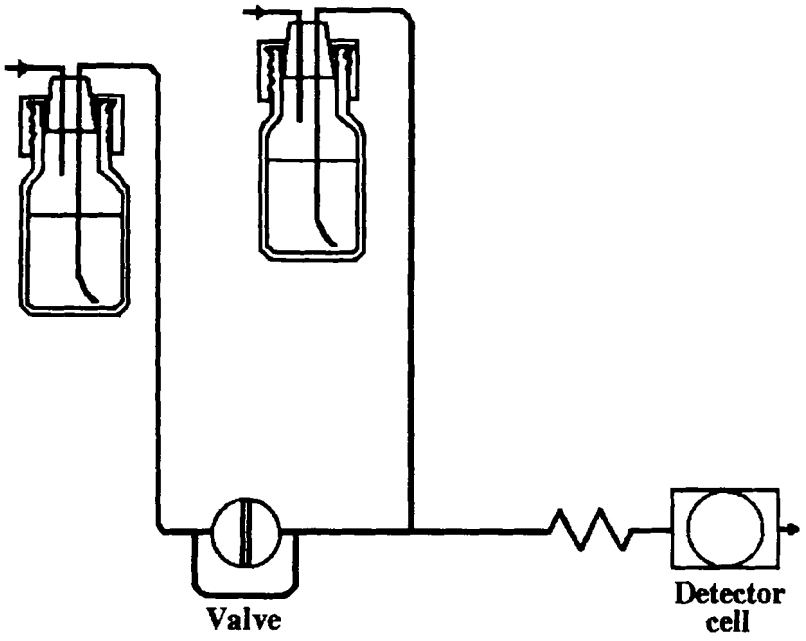

FIGURE 24. Two-channel system for on-line sample manipulation. (From Frenzel, W.; Bratter, P. *Anal. Chim. Acta.* **1986,** *179,* 389–398. With permission.)

treatment. Frenzel et al. checked for the theoretical prediction of the FIPSA technique of a linear signal dependence on the residence time of the sample; they used times in the 0.5- to 600-s range and different injection volumes, flow rates, and metal ion concentrations. The prediction was found to hold for all four types of cell. In contrast to the theoretical predictions for flow-injection anodic stripping voltammetry, the stripping time in FIPSA is inversely proportional to the flow rate as long as this is not altered between deposition and stripping. This is a result of the increased plating efficiency at high flow rates being offset by the likewise faster transport of oxidant during stripping. In all cases, experimental verification was obtained for flow rates in the 0.2- to 6-ml/min range except for the open thin-layer cell, where the maximum useful flow rate was 2 ml/min (the filter strip was flushed away at higher flow rates). The question of which cell was best suited for FIPSA could not be answered unambiguously, however. The shape and length of the stripping curves were nearly identical under comparable experimental conditions. With respect to responsiveness and carryover, the laboratory-made wall-jet cell proved superior. For practical reasons, the open thin-layer cell (Figure 25) was found to be preferable because disassembling for cleaning and removing air or hydrogen bubbles was obviously unnecessary.

Locascio and Janata[77] designed and tested an automatic system for the determination of lead(II) and cadmium(II) in the 10^{-3} to 10^{-6} *M* range. It consisted of solid-state integrated circuitry containing a chemically sensitive field-effect transistor (CHEMFET) and a transistor control switch (Figure 26). Flow of solutions, application of potentials during the electrode preparation, plating and stripping periods, and data acquisition were controlled by an inexpensive microprocessor. Sample volumes of 200 µl containing the metals at concentrations in the above-mentioned range could be processed in less than 2.5 min with a relative standard deviation below 10%. The detection limit was at

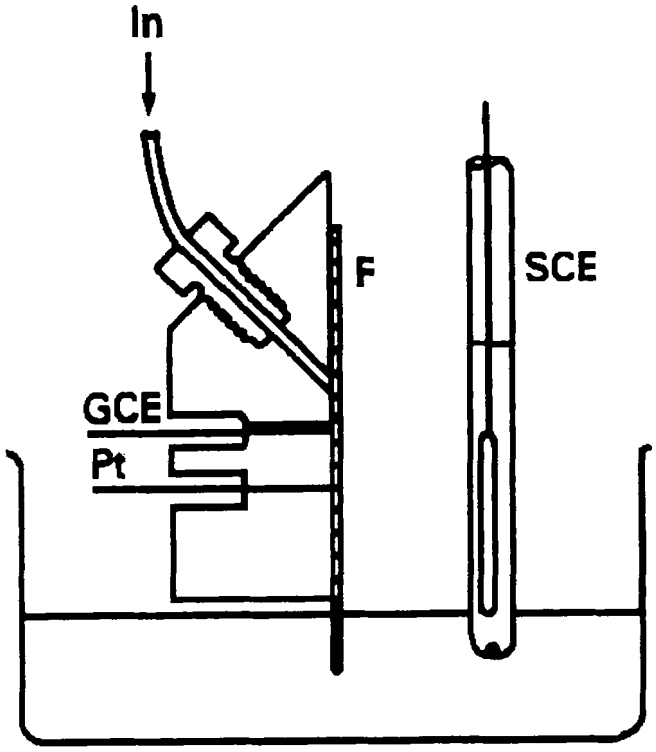

FIGURE 25. Schematic diagram of open thin-layer cell. GCE, 1 mm glassy carbon working electrode; Pt, 0.2-mm auxiliary electrode; SCE, saturated calomel reference electrode; F, filter strip. (From Frenzel, W.; Schulze, G. *Analyst.* **1987,** *112,* 133–136. With permission.)

the time restricted by the low sampling rate of the microprocessor used (a Commodore VIC20). Also, the upper value of the usable concentration range was limited by the maximum practical concentration of oxidant.

An electrochemical flow-cell suitable (Figure 27) for use with dual detection by PSA and atomic absorption spectrometry in a flow injection system was characterized by Schulze from its flow pattern and dispersion measurements.[78] The deposition efficiency could be altered from 1 to 2% to 24% by using a glassy carbon and a carbon felt electrode, respectively. Application to the determination of lead in water showed that, after enrichment on carbon felt, the sensitivity for flame atomic absorption spectrometry was increased by one order of magnitude (enrichment factors of ~5 and ~30 at sampling frequencies of 60 and 12 h^{-1}, respectively). Dual detection allowed some errors arising from apparatus malfunctioning or a wrong sample treatment in one of the methods to be identified, thus providing accuracy checks.

Matuszewski et al.[31] reported an FIPSA system using an IBM PC/XT computer for rapid digital recording of potential-time curves. A straightforward high-volume wall-jet cell[79] was used as detector cell (Figure 28). Investigations of the influence of electrode pretreatment and solution delivery mode (i.e., by gravity flow, pumping, etc.) revealed these parameters to have a significant effect on the magnitude and precision of stripping times. The optimized system was applied to the simultaneous determination of cadmium and lead in geological samples.

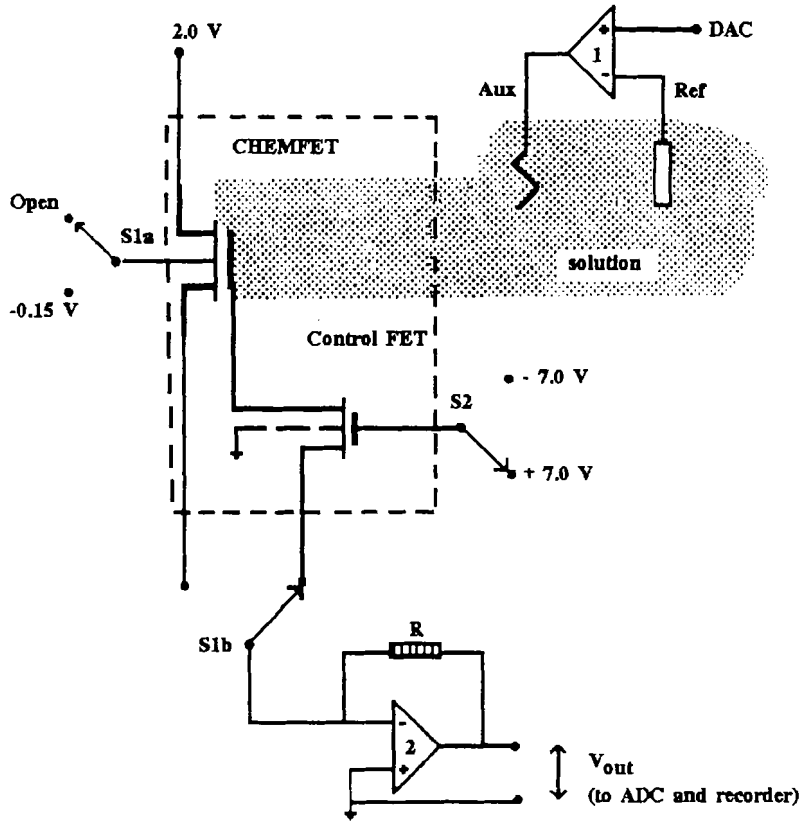

FIGURE 26. Circuit diagram of the integrated potentiometric stripping system. The auxiliary electrode (Aux) is connected to the output of operational amplifier 1 and supplies the necessary current to maintain a constant potential on the reference electrode (Ref). A D/A converter that is connected to the positive input of the same amplifier sets the potential of the reference electrode. S1a and S1b are switched by a DPTD relay, and S2 is switched independently by an SPDT relay. When S1a, S1b, and S2 are in the positions shown in the diagram, the CHEMFET is in the plating mode. When S1a, S1b, and S2 are in their alternative positions, the CHEMFET is in the stripping mode. The output voltage of operational amplifier 2 is recorded during the stripping cycle. The value of feedback resistor R is 25.9 kΩ. The part of the circuit inside the dashed line area is on one integrated silicon chip. (From Locascio, L.E.; Janata, J. *Anal. Chim. Acta.* **1987,** *194,* 99–107. With permission.)

VI. INTERFERENCES IN POTENTIOMETRIC STRIPPING ANALYSIS

PSA interferences can be classified into two broad categories: those arising from the presence of metals and those introduced by organic substances in the samples.

The interferences posed by metals can in turn be classified into four groups:[80]

1. Class 1 interferences arise from interferents, I, that decreased the analytical signal of the analyte, A, through a parallel oxidative action of ionic I toward the deposited A. Obviously, I must be a stronger oxidant than A in

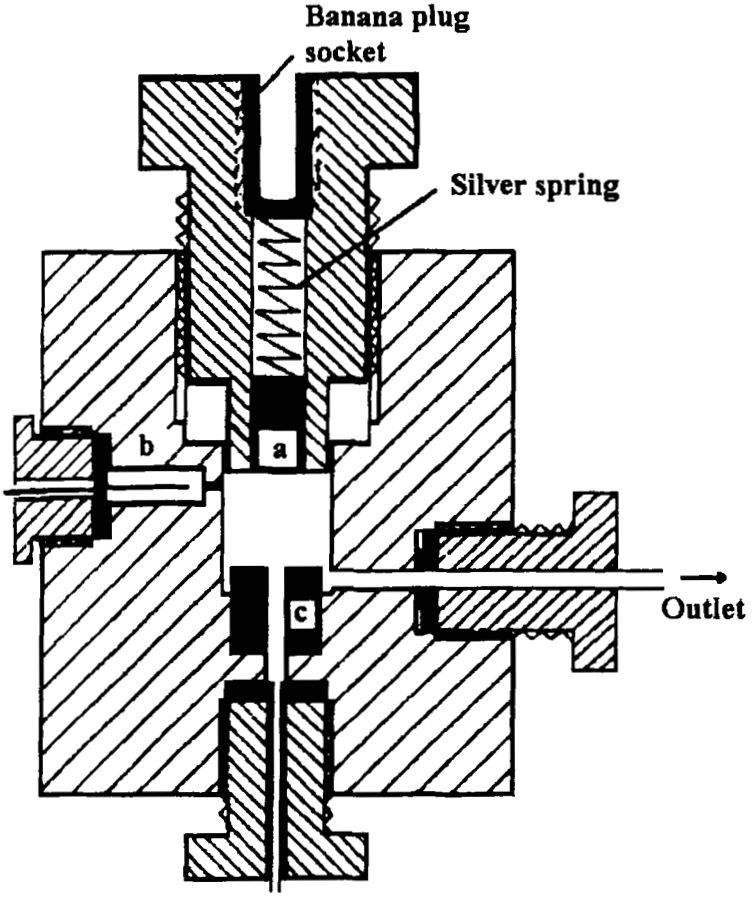

FIGURE 27. Flow-through cell for potentiometric stripping analysis. (a) working electrode; (b) reference electrode; (c) auxiliary electrode. (From Schulze, G.; Koschany, M.; Elsholz, O. *Anal. Chim. Acta.* **1987,** *196,* 153–161. With permission.)

the given ionic medium. The following reactions take place in parallel during the stripping of A:

$$A(Hg) + (n/2)\,Hg^{2+} \rightarrow A^{n+} + (n/2)\,Hg(I) \quad (47)$$

$$m\,A(Hg) + n\,I^{m+} \rightarrow m\,A^{n+} + n\,I(Hg) \quad (48)$$

where M(Hg) denotes amalgamated M.

The magnitude of the signal decrease will depend on the relative reaction-rate constants of the heterogeneous Reactions 47 and 48, and the $[I^{m+}]/[Hg^{2+}]$ ratio.

The proportionality between the analyte concentration is generally preserved. Typical cases of class 1 interferences are observed with the following A-(I_1,I_2, . . .) pairs: Zn-(Cd, Tl, In, Pb, Bi), Ga-(Cd, Tl, Pb), Cd-(Pb, Bi), Tl-(Pb, Cu, Bi), In-(Pb, Cu, Bi), Pb-(Cu, Bi), and Cu-Bi. On the other hand, no class 1 interferences have been detected for Zn-(In, Pb) in 0.1 *M* HCl.

2. Class 2 is only observed if I is less oxidant than A and is capable of being plated, giving a stripping plateau preceding that of A. An increase in the analytical signal is observed that can be attributed to the direct reduction of A^n

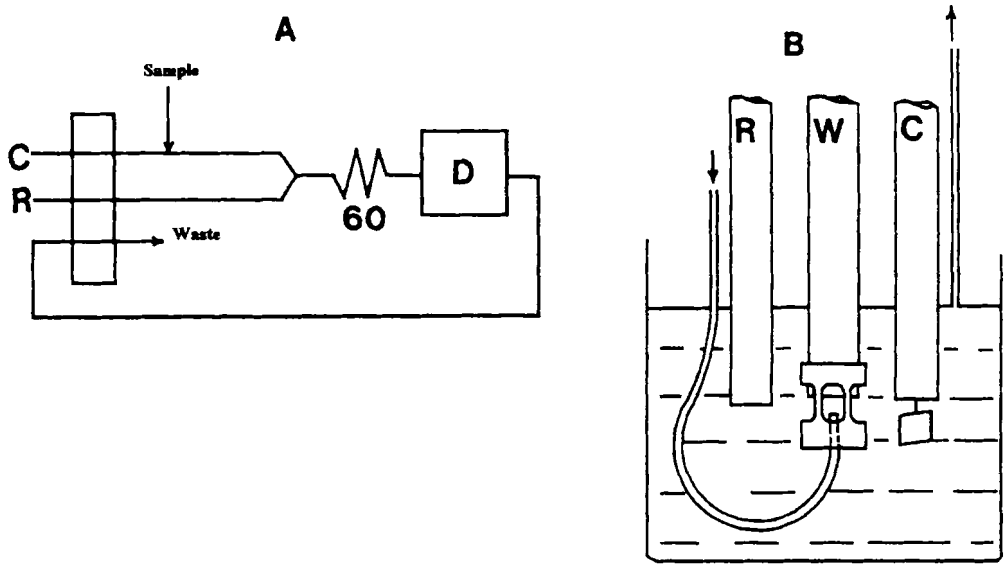

FIGURE 28. (A) Manifold used in flow injection measurements. C, carrier solution; R, reagent solution; D, detector cell. (B) Configuration of the measuring cell in flow injection measurements. W, glassy carbon working electrode with perpex cap in wall-jet arrangement; R, reference electrode; C, counter electrode. (From Matuszewski, W.; Trojanowicz, M.; Frenzel, W. *Fresenius Z. Anal. Chem.* **1988,** *332,* 148–152. With permission.)

at the electrode surface by amalgamated I, which takes place in two simultaneous reactions during the stripping of I:

$$I(Hg) + (m/2)\ Hg^{2+} \rightarrow I^{m+} + (m/2)\ Hg \quad (49)$$

$$n\ I(Hg) + m\ A^{n+} \rightarrow m\ A(Hg) + n\ I^{m+} \quad (50)$$

In most instances, for the same time interval, Reaction 50 yields larger amounts of A(Hg) during the stripping of I than does the following reaction during the deposition step:

$$A^{n+} + n\ e^{-} \rightarrow A(Hg) \quad (51)$$

In contrast to class 1 interferences, class 2 interferences may be readily suppressed or completely circumvented by a judicious choice of the deposition potential. Thus, using a deposition potential between the stripping potentials of I and A will prevent deposition of the former.

The proportionality between the analytical signal and the analyte concentration is generally preserved unless other classes of interferences are involved.

Typical class 2 interferences are observed with the following pairs: Cd-Zn, Tl-Zn, In-Zn, Pb-(Zn, Cd, In), Cu-(Zn, Cd, In, Pb, Tl), and Bi-(Zn, Cd, Tl, In, Pb).

3. Class 3 interferences are observed when A and I form one or more intermediate compounds. These interferences are readily distinguished from class 1 and class 2 interferences because, in most cases, they appear at relatively low interferent concentrations. They usually result in a dramatic decrease in the

analytical signal. An increased signal is to be expected, however, if the intermetallic compound is stripped at the same potential as the analyte. Intermetallic compounds are known to behave as separate metals and are reportedly oxidized at potentials between the oxidation potentials of the individual metals or at the same potential as one of the constituent metals.[81]

In the presence of low interferent concentrations, the analytical signal is linearly related, but not proportional, to the analyte concentration because either part of the analyte is consumed by the interferent to form the intermetallic compound or this is stripped together with the analyte. The analytical signal decreases or increases by a constant amount that is proportional to the interferent concentration.

Typical instances of class 3 interferences with a decrease in the analytical signal are observed with the following pairs: Zn-(Cu, Ni, Co), Ga-(Cu, Ni, Co, Zn), and Cd-(Cu, Ni, Co), while a signal increase is observed with the Cu-Zn pair. This can only be partly ascribed to a class 3 interference, as the predominant interference is of class 2.

4. Class 4 interferences encompass all interactions not amenable to classes 1 through 3. They may originate from various phenomena:

   A. Chemical interaction between A and I prior to the deposition step (e.g., inhibition of the deposition of A by coprecipitation with basic salts of I). Typical instances are observed with the following pairs: Zn-[Cr(III), Al] in acetate buffer at pH 4.0, Ga-[Cr(III),Al], Cd-[Cr(III), Al], Tl-[Cr(III), Al, Ga)], and In-(Al, Ga). In all cases, addition of the interferent after the deposition step has virtually no effect on the analytical signal.

   B. Formation of a separate crystalline phase of I on the surface of the mercury layer may also considerably influence the analytical signal in either direction. In most cases, E-t recordings are accompanied by noise that obscures the signal. Typical instances are observed with the following pairs: Tl-(Ni, Co), In-(Ni, Co), Pb-(Ni, Co), and Bi-Ni.

   C. Interferences observed mainly with Ca, Mg, and Mn are not amenable to either of the above described phenomena. Such interferences are observed with the following pairs: Zn-(Mn, Ca, Mg), Ga-(Mn, Ca, Mg), Tl-(Ca, Mg), Bi-Al, and Bi-Cu — this is in contradiction with class 1 Cu-Bi, as α-class 2 Bi-Cu would be expected).

Not only the proportionality, but also the linearity between the analytical signal and the analyte concentration seem to be affected by class 4 interferences. The relationship between the analytical signal and the analyte concentration should be checked in each separate instance.

It should be stressed that mixed-classed interferences are also likely to occur. One typical example is the Cd-Ga pair, where class 2 and 3 interferences may compete with each other, resulting in an unusual, consistently nonmonotonic interference pattern.

The specialized literature includes various procedures for the elimination of interferences due to the presence of metals. Thus, Danielson et al.[82] overcame the strong interference of copper in the determination of zinc by adding gallium, which forms a more stable intermetallic compound with copper, thus allowing zinc to be oxidized at its normal stripping potential. Copper(II) can thus be determined in the presence of zinc following deposition at a potential where Zn(II) is not reduced.

Hoyer and Kryger[83] used the generalized standard-addition method (GSAM) to resolve overlapping signals and correct those affected by the formation of intermetallic intermediates because the normal SAD provided inaccurate results if the analytical stripping signal was overlapped by one or more signals resulting from the stripping of nonanalyte components. In addition, if an amalgamated metal takes part in the formation of an intermetallic compound with plated nonanalyte components, care should be exercised to eliminate this effect prior to application of the normal SAD.

On the other hand, these interferences can readily be overcome in many cases. Nearly coincident stripping signals can often be well resolved by using another medium; also, their relative magnitudes can many times be controlled via the plating conditions. Flow techniques with medium exchange provide an additional means for controlling the selectivity.

As regards the interferences posed by the presence of organic matter (OM) in PSA, the technique is much less markedly affected by adsorbed OM than are other stripping techniques such as ASV because, when OM covers the electrode, the diffusion of both the metal ion and the oxidant are similarly hindered, so the effects tend to cancel each other out. Moreover, organic redox compounds do not interfere with the analysis, so measurements of the electroactive fraction of the metal can be performed in complex media, which results in less complicated sample pretreatments.

The adsorption of proteins and surfactants or the accumulation of reaction products at the electrode surface can result in a gradual loss of electrode activity when a mercury electrode is used for the determination of heavy metals in complex mixtures. Obvious ways of improving the selectivity in PSA include using modified electrodes to protect their surfaces from adsorptive interferences, a matrix-modifying solution, or the SAM in the analyses.

With voltammetric techniques, soluble reversible redox couples may pose interference problems. The equilibrium concentrations of such couples at the working electrode are determined by the controlled electrode potential according to the Nernst equation. When the electrode potential exceeds the characteristic potential of the couple, a rapid, transport-controlled redox conversion takes place and a Faradaic signal is obtained as a result. Reversible couples may often exist as intermediate products when natural samples containing traces of organic matter are subjected to voltammetric analysis. With pulse voltammetric techniques, where rapid potential steps are employed, the effect is more pronounced than with slow potential sweeps.

In PSA, where the sample contains excess oxidant, dissolved reversible couples only exist while potentiostatic control is maintained (i.e., during the plating period). During stripping, when potentiostatic control is abandoned, only the oxidized form can exist, the reduced form being converted so rapidly that no characteristic plateau or peak is observed. The transport rate of oxidant toward the working electrode is of little consequence here because the reduced form is not preplated on the electrode and therefore is at a low concentration relative to the concentration of oxidant immediately available at the electrode. Nevertheless, the analytical signal may be decreased as a result of the organic compound concerned having a reduction potential similar to the analyte oxidation potential. The decrease is usually insignificant, provided the SAM is used for quantitative work.

VII. APPLICATIONS OF POTENTIOMETRIC STRIPPING ANALYSIS

PSA is not as general an analytical technique for the determination of metal traces as is graphite-furnace atomic absorption spectroscopy, for example. However, in samples

containing high concentrations of inorganic salts, the PSA technique seemingly surpasses spectroscopic techniques for the determination of some elements. Typical samples are body fluids, mineral acid digests from biological materials, saline waters, and chemicals for purity testing. Table 1 summarizes selected applications reported after the literature review by Jagner[14] was published. Of special note in this context is the recent work of Ostapczuk et al.[6,84] and Labar,[85] who assessed the present potential and limitations of the determination of trace elements by PSA in various types of samples of both clinical and environmental interest, and reported the results obtained in interlaboratory quality-control experiments.

A second area of application for PSA is the determination of the different chemical forms of trace elements in samples,[14] in common with nearly every electroanalytical technique. By proper adjustment of the potentiostatic deposition potential, the working electrode can be made to respond only to hydro or chloro complexes of the trace metal and not to the EDTA complex, for example. Applications of this type include those reported by Jagner and Aren[86] and Fayyad,[87] who determined the conditional stability constants for the EDTA complexes of Pb(II) and Bi(III), and the dissociation potentials of the Bi-NTA and Bi-EDTA complexes (NTA denotes nitrilotriacetic acid), respectively, using computerized flow-injection.

The PSA technique can also be used as a complementary analytical technique in conjunction with atomic absorption spectroscopy for analysis of a wide variety of samples in order to comply with the results dictated by national legislation boards, which are increasingly demanding that samples be analyzed by two different analytical techniques. For many toxic trace metals, PSA seems to be the best complement.

TABLE 1
Selected Applications Reported After the Literature Review by Jagner[14] Was Published

Elements	Sample	Aut[a]	Contrast	Interval (precision)	L. O.D., dep. time[b]	Electrode	Comments	Ref.
Cu, Pb	Sediments	Yes	RM	3–110 μg/g Cu 7–700 μg/g Pb (4%)		GCMF	Cd as internal standard; He as deareating gas	88
Pb, Sn	Fruit juices, soft drinks	Yes	AAS, ASV	(5%)	1 μg/l, 16 min	GCMF	Methanol as supporting electrolyte; N_2 as deareating gas	89
Zn, Cd, Pb, Cu	Potable water						O_2 as oxidant	90
Zn	Waste water						Ga as Cu scavenger	91
Cd, Pb, Zn	Synthetic	No	None	0.1–1 μg/g (5%)		CF (4 kinds)	DPASV also studied; not deareated	38
Pb, Cd, Zn	Synthetic	No	None	(0.5%, Pb, Cd) (4.5%, Zn)	2×10^{-10} *M* Cd, 5 min	GCMF	Uranium(VI) does not interfere	92
Cu, Pb, Cd, Zn	Seawater	Yes	AAS, ICP	(2–5%)		GCMF	N_2 as deareating gas	93
Cu, Bi, Sb, Pb	Fruit leaf, water		AAS, ES	(5)	5 μg/ml, 20 min	GCGF	Gold(III) as oxidant	94
Cu, Pb, Zn	Canned food				Sn 0.1 μg/g Pb, Cu 0.01 μg/g			95
Cu	Steel		CS	0.1–25 μg/ml	0.05 μg/ml		Sample as oxidant	96
Pb	Milk						No pretreatment needed	97
Pb, Tl	Seawater	No	Std. add.	5×10^{-8}–10^{-5} *M* (2%)		GCMF	Concentration ratios 1:100 to 100:1	98
Sn	Rocks		PCR			GCGF	Gold (III) as oxidant	99
Cu, Pb	Environmental			(5%)		Pt		100
Cr	Tapwater	—		0–50 μg/l		GCMF		101
Pb, Cu	Milk	—		(2.8%)	3 ng, 16 min	GCMF		102
Cu	Wine	Yes	AAS	(2–8%)		GCMF	Treatment with NO_3H	103
Oxygen (O_2)	Waters	No	Winkler	(3%)	<0.4 mg/l	GCMF	Cd(II) is reoxid. by O_2	104
Cd, Pb, Cu	Synthetic	No	None	10^{-7}–10^{-5} *M* (10%)	ca. 10^{-9} *M*, 10 min	CF and Au μ-electrodes	μ-samples; Ar as deareating gas	39
Cd, Pb, Cu	Milk, milk powder	Yes	RM	0.1–5 μg/l Cd, 1–20 μg/l Pb, 5–100 μg/l Cu (5–7%)	1 μg/l Cd, 4 min 4 μg/l Pb, 1 min 8 μg/l Cu, 30 s	GCMF	Flow analysis; Pb in high Zn content samples	28
Tl	Coal fly-ash	Yes	RM	(10%)		GCMF	Sample acts as oxidant	30
Cd, Cu, Zn	Seawater	—	ASV	(1%)				106
Pb, Cd	Teeths	—	AAS				Pb higher in urban areas	107
Oxygen (O_2)	Water	No	O_2 Se, Winkler	(2%)		GCMF	Cd(II) reoxid. by O_2	108
Pb, Cd	Biological	—	RM, DPASV	(2–10%)		HMDE	N_2 as deareating gas	109

Pb	Urine	Yes	RM	(9%)		CF	Flow analysis	61
NTA	Water (waste, natural)	No	None	(1, 5%)		GCMF	Bi(III) is complexed; Dichromate as oxidant	110
Mo(VI)	Seawater	Yes	RM	0–20 μg/l (15%)		GCMF	Complex with 8-Quinolone	58
Cd, Pb	Whole blood	Yes	RM, AAS	(15%, Pb), (2%, Cd)		CF	Flow analysis	62
Cd, Pb	Synthetic	Yes	None	0.01–10 mg/l (5–10%)		CF	μ-cell (5–20 μl); Ar as deareating gas	40
Bi	Atmospheric partic.	—					SCN complexes Bi.	111
Cu, Pb	H_2O_2	—		(5%)	10 μg/l, 10 min			112
Zn	Plasma	—	AAS	0.02–1 μg/g	3 μg/l			113
Iodide	Lavers	—		(3.3%)	10^{-10} *M*	MF	CuI precipitated is reox. by Fe(III)	114
EDTA	Water	No	None	(2.5%)	1 μg/l, 3 min	GCMF	Bi(III) complex/dichromate as oxid.	115
Pb, Zn, Cd	Urine	Yes	RM	(9%)		Nafion	Biological surfactants don't interfere; flow analysis	116
As	Urine, seawater	Yes	RM	1–100 μg/l (5%)	0.1 μg/l, 1 min	GCPF	Electro and chemical (Au(III)) oxidation; FI	63
Pb	Whole blood	—		(3.4%)	0.0009 μg/ml			117
Pb	Soy sauce	—		(10%)				118
Cu, Pb	Wine	—		(2%)			Interrupted multiple scan	119
Cd, Cu, Pb	Glucose, agar	—						120
Sc	—	—		Rec. 99.8%	2×10^{-8} *M*		Stability EDTA-Cd vs. EDTA-Sc	121
As	Sb trioxide	—		0–110 μg/l		GCMF	As is extracted	123
Ni	Synthetic	No	None	(1.7%)	8 μg/l, 1.5 min	DMG-GP	Nondeareated	43
Zn	Brass	Yes	RM with high Cu	(10%)		GCMF	Gas as Cu scavenger; N_2 as deareating gas	105
In	Sphalerites	Yes	Std. add.	(10–14%)		GCMF	Separation step required	123
Cu, Pb		No		(3–11%)		GCMF		20
Pb	Urine	—	Dithizone method	0–150 μg/l (1.6%)	2 μg/l	GCMF		124
Hg	Fish	—		Rec. 97%			MnO_4, Cu(II), electrode as oxidant	125
Pb	Urine	—		(3–6%)	2 μg/l			126
Cd, Cu, Pb	Grains	—					KCl as electrolyte	127
Cu, Hg	Conch	—	AAS	Rec. 102% Hg, 97% Cu	2×10^{-10} *M*		MnO_4 as oxidant	128
Cd, Pb	Synthetic	Yes	None			GCMF		150
Cd, Cu, Pb, Zn	Synthetic	Yes	None	0.02–0.35 μg/g Zn; 0.08–0.4 μg/g (5–12%)		GCMF	O_2 as oxidant	32
Hg	Synthetic	Yes	None	0.4–1.6 μg/g (7%)		Gold	Kinetic determination; $IO_4^{-/}$– as oxidant	11
Bi	Water	—		(3%)	5×10^{-10} *M*	Nafion		129
Hg	Water, air	—	AAS	0–100 μg/l, rec. 94%		GCMF	MnO_4, Cr(VI) oxidants	130
Cu, Cd, Pb, Zn	Grain	—		Rec. 86–106%				131
Hg	Synthetic	Yes	None	40–800 μg/l (5%)		Gold	Kinetic determination; CCO	33

TABLE 1 (continued)
Selected Applications Reported After the Literature Review by Jagner[14] Was Published

Elements	Sample	Aut[a]	Contrast	Interval (precision)	L. O.D., dep. time[b]	Electrode	Comments	Ref.
Cd, Pb	Plants	—		Rec. 115%				132
Cl species	Synthetic	Yes	None	0.025–2 mg/l (3%)	0.07 mg/l	Gold film	Flow analysis	35
Reducing sugars	Beverages, wines, honey, marmalades	Yes	AOAC method	10^{-3}–10^{-2} *M* (1–6%)		GCMF	Determination of Cu(II) not reduced	133
Ge	Garlic, mineral waters	No	FIPSA, ASV	(1–10) × 10^{-8} *M*	8.5 × 10^{-9} *M*, 15 min	GCMF	Sensitivity enhanced by ARS	37
Ni, Mn, K, Na, Li	Synthetic	Yes	VSA			CF and gold	Various solvents	134
Pb	Synthetic	Yes		(1–4.5) × 10^{-5} *M*		GCMF	Fe(III) as oxidant	21
Zn	Blood serum	—						135
Cu	Preserved egg	—	AAS	Rec. (97%)	2 × 10^{-10} *M*	GC	O_2 as oxidant	136
Cd, Cu, Mn, Pb, Zn	Water, biological	—	AAS				Mn is determined if p-ABS acid is added.	137
Co	Steel	—		0.5 ng/l–0.2 µg/l	0.1 ng/l	HMDE	DMG-Co is adsorbed on the electrode	138
Fe	Wine	—		0–150 µg/l	5 µg/l, 5 s	GCMF	CCO	140
Cd, Pb	Whole blood	—			1 µg/l, 1 min			141
Ge	Wine	—		Rec. 95–106%		GF		142
Pb	Flour	Yes		(7.7%)				143
Pb	Drinking water	Yes	None	0–100 µg/l (3%)	0.3 µg/l	CSP		47
Pb	Wines	Yes	AAS, ASV	(3–7%)		GCMF	Wine digested	144
Pb	Gasoline	Yes	AAS	(4–8%)	0.07 mg/l	GCMF	Organolead determined	5
Cd	Synthetic	No	None	0.1–1 µ *M* (3–8%)		GCM	CCO	48
Cd, Pb	Blood	Yes					Flow analysis	9
As	Human hair	—					Flow analysis	145
Pb	Whole blood	—		Rec. 110%	4.3 × 10^{-6} m*M*			146
Pb	Urine, water	Yes	None	5–250 µg/l	0.1 µg/l Pb 20	Gold-coated CSP		147
Pb 84	Wines	Yes	AAS	(4–7%)		GCMF		
Cd, Pb, Cu	Synthetic	Yes	None	(2–3.5%)		GCMF		85
Cd, Pb	Urine, water (spiked)	Yes	None	(4–5%)		CM-GCMF	CCO; effect of surfactants studied	3
Cu, Pb	Water	Yes	AAS	0.10–5 mg/l Cu; 1–50 µg/l Pb; (15%)	100 µg/l Cu, 1 min; 1 µg/l Pb, 3 min	GCMF		148

Cd, Cu, Pb, Zn	Seawater	—	(3–6%)	0.02 µg/l Zn, Cu; 0.01 µg/l Cd; 0.006 µg/l Pb; 10 min	No pretreatment required	149

Note: AAS, atomic absorption spectroscopy; p-ABS acid, *p*-aminobenzenesulfonic acid; ARS, alizarin red; ASV, anodic stripping voltametry; CCO, constant current oxidation; CF, carbon fiber electrode; CGF, carbon gold film; CM-GCMF, cellulose acetate membrane GCMF electrode; CS, conventional spectroscopy; CSP, carbon screen-printed electrode; DMG, dimethylglyoxime; DMG-GP dimethylglyoxime-containing graphite paste electrode; DPASV, differential impulsional ASV; ES, emission spectroscopy; FIPSA, flow injection PSA; GC, glassy carbon electrode; GCGF, glassy carbon gold film electrode; GCMF, glassy carbon mercury film electrode; GCPF, gold-coated platine fiber; HMDE, hanging mercury drop electrode; ICP, inductively coupled plasma; MF, mercury film electrode; NTA, nitriloacetic acid; PCR, polarography cathode-ray; RM, reference material; SE, selective electrode; VSA, voltammetric stripping analysis.

[a] Automated.
[b] Deposition time; L.O.D., limit of detection.

REFERENCES

1. Jagner, D.; Graneli, A. *Anal. Chim. Acta.* **1976,** *83,* 19–26.
2. Jagner, D.; Aren, K. *Anal. Chim. Acta.* **1978,** *100,* 375–388.
3. Aldsstadt, J. H.; Dewald, H. D. *Anal. Chem.* **1993,** *65,* 922–926.
4. Renman, L.; Jagner, D.; Berglund, R. *Anal. Chim. Acta.* **1986,** *188,* 137–150.
5. Jagner, D.; Renman, L.; Wang, Y. *Anal. Chim. Acta.* **1992,** *267,* 165–169.
6. Ostapczuk, P. *Anal. Chim. Acta.* **1993,** *273,* 35–40.
7. Mortensen, J.; Ouziel, E.; Skoy, H.; Kryger, L. *Anal. Chim. Acta.* **1979,** *112,* 297–312.
8. Kryger, L. *Anal. Chim. Acta.* **1980,** *120,* 19–30.
9. Zie, Y.; Huber, C. O. *Anal. Chim. Acta.* **1992,** *263,* 63–70.
10. Jin, W.; Wang J. *Anal. Chim. Acta.* **1991,** *252,* 59–64.
11. Cladera, A.; Estela, J. M.; Cerdà, V. *J. Electroanal. Chem.* **1990,** *288,* 99–109.
12. Christensen, J. K.; Kryger, L. *Anal. Chim. Acta.* **1980,** *118,* 53–64.
13. Christensen, J. K.; Kryger, L.; Mortensen, J.; Rasmussen, J. *Anal. Chim. Acta.* **1980,** *121,* 71–83.
14. Jagner, D. *Analyst.* **1982,** *107,* 593–599.
15. Chau, T. C.; Li, D.; Wu, Y. L. *Talanta.* **1982,** *29,* 1083–1087.
16. Mortensen, J.; Britz, D. *Anal. Chim. Acta,* **1981,** *131,* 159–165.
17. Labar, C.; Lamberts, L. *Anal. Chim. Acta.* **1981,** *132,* 23–33.
18. Hussam, A.; Coetzee, J. F. *Anal. Chem.* **1985,** *57,* 581–585.
19. Hoyer, B.; Kryger, L. *Talanta.* **1985,** *32(9),* 839–844.
20. Xia, Y. H.; Chou, T. C.; Mo, J. Y. *Anal. Chim. Acta.* **1989,** *222,* 263–268.
21. Labar, C.; Muller, R.; Lamberts, L. *Electrochim. Acta.* **1991,** *36(14),* 2103–2108.
22. Garai, T.; Mészáros, L.; Bartalits, L.; Locatelli, C.; Fagioli, F. *Electroanalysis.* **1991,** *3,* 955–961.
23. Vries, W. T.; Van Dalen, E. *J. Electroanal. Chem.* **1964,** *8,* 366.
24. Vries, W. T.; Van Dalen, E. *J. Electroanal. Chem.* **1967,** *14,* 315.
25. Garai, T.; Nagy, Z.; Mészáros, L.; Bartalits, L.; Locatelli, C.; Fagioli, F. *Electroanalysis.* **1992,** *4,* 899–904.
26. Graneli, A.; Jagner, D.; Josefson, M. *Anal. Chem.* **1980,** *52,* 2220.
27. Hu, A.; Dessy, R. E.; Graneli, A. *Anal. Chem.* **1983,** *55,* 320.
28. Almestrand, L.; Jagner, D.; Renman, L. *Talanta.* **1986,** *33,* 991.
29. Hoyer, B.; Kryger, L. *Talanta.* **1986,** *33,* 883.
30. Hoyer, B.; Skov, H. J.; Kryger, L. *Anal. Chim. Acta.* **1986,** *188,* 205.
31. Matuszewski, W.; Trojanowics, M.; Frenzel, W. *Fresenius Z. Anal. Chem.* **1988,** *332,* 148–152.
32. Cladera, A.; Estela, J. M.; Cerdà, V. *J. Autom. Chem.* **1990,** *12,* 108–112.
33. Cladera, A.; Estela, J. M., and Cerdà, V. *Talanta.* **1991,** *38,* 1475–1479.
34. Jagner, D. *Anal. Chim. Acta.* **1979,** *105,* 33–41.
35. Xie, Y.; Huber, C. O. *Anal. Chem.* **1991,** *63,* 208–212.
36. Jagner, D.; Josefson, M.; Westerlung, S. *Anal. Chem.* **1981,** *53,* 2144–2146.
37. Dexiong, F.; Peihui, Y.; Zhaoliang, Y. *Talanta.* **1991,** *38(12),* 1493–1498.
38. Schulze, G.; Frenzel, W. *Anal. Chim. Acta.* **1984,** *159,* 95–103.
39. Baranski, A. S.; Quon, H. *Anal. Chem.* **1986,** *58,* 407–412.
40. Frenzel, W. *Anal. Chim. Acta.* **1987,** *196,* 141–152.
41. Kapauan, A. F. *Anal. Chem.* **1988,** *60,* 2161–2162.
42. Albery, W. J.; Bruckenstein, S. *J. Electroanal. Chem.* **1983,** *144,* 105–112.

43. Trojanowicz, M.; Matuszewski, W. *Talanta.* **1989,** *36(6),* 680–682.

44. Huiliang, H.; Jagner, D; Renman, L. *Anal. Chim. Acta.* **1988,** *207,* 17–26.

45. Aldstadt, J. H.; Dewald, H. D. *Anal. Chem.* **1992,** *64,* 3176–3179.

46. Martins, E.; Bengtsson, M.; Johansson, G. *Anal. Chim. Acta.* **1985,** *169,* 31–42.

47. Wang, J.; Tian, B. *Anal. Chem.* **1992,** *64,* 1706–1709.

48. Wang, J.; Tian, B. *Anal. Chem.* **1993,** *65,* 1529–1532.

49. Anderson, L.; Jagner, D.; Josefson, M. *Anal. Chem.* **1982,** *54,* 1371–1376.

50. Hanekamp, H. B.; Van Niewkerk, H. J. *Anal. Chim. Acta.* **1980,** *121,* 13–22.

51. Levich, V. G. *Physicochemical Hydrodynamics.* Prentice-Hall: Engelwood Cliffs, N. J., 1962.

52. Swartzfager, D. G. *Anal. Chem.* **1976,** *48,* 2189–2192.

53. Jagner, D.; Josefson, M.; Aren, K. *Anal. Chim. Acta.* **1982,** *141,* 147–156.

54. Mannino, S. *Analyst.* **1984,** *109,* 905–907.

55. Eskilsson, H.; Turner, D. R. *Anal. Chim. Acta.* **1984,** *161,* 293–302.

56. Dyrssen, D.; Eskilsson, H.; Haraldsson, C. *J. Electroanal. Chem.* **1989,** *262,* 161–165.

57. Almestrand, L.; Jagner, D.; Renman, L. *Talanta.* **1986,** *33(12),* 991–995.

58. Hua, C.; Jagner, D.; Renman, L. *Anal. Chim. Acta.* **1987,** *192,* 103–107.

59. Huiliang, H.; Hua, C.; Jagner, D.; Renman, L. *Anal. Chim. Acta.* **1987,** *193,* 61–69.

60. Jennings, V. J.; Morgan, J. E. *Anal. Proc.* **1983,** *20,* 276.

61. Huiliang, H.; Jagner, D.; Renman, L. *Talanta.* **1987,** *34(6),* 539–542.

62. Almestrand, L.; Jagner, D.; Renman, L. *Anal. Chim. Acta.* **1987,** *193,* 71–79.

63. Huiliang, H.; Jagner, D.; Renman, L. *Anal. Chim. Acta.* **1988,** *207,* 37–46.

64. Huiliang, H.; Jagner, D.; Renman, L. *Anal. Chim. Acta.* **1988,** *207,* 27–35.

65. Huiliang, H.; Hua, C.; Jagner, D.; Renman, L. *Anal. Chim. Acta.* **1988,** *208,* 237–246.

66. Huiliang, H.; Jagner, D.; Renman, L. *Anal. Chim. Acta.* **1988,** *208,* 301–306.

67. Hua, C.; Jagner, D.; Renman, L. *Talanta.* **1988,** *37(7),* 525–529.

68. Hu, A.; Dessy, R. E.; Granéli, A. *Anal. Chem.* **1983,** *55,* 320–328.

69. Buffle, J.; Pelletier, M.; Monnier, D. *J. Electroanal. Chem.* **1973,** *43,* 185.

70. Brukenstein, S.; Bixier, J. W. *Anal. Chem.* **1965,** *37,* 786.

71. Bixier, J. W.; Bruckenstein, S. *Anal. Chem.* **1965,** *37,* 391.

72. Jagner, D. *Anal. Chem.* **1978,** *50,* 1924.

73. Jagner, D. *Anal. Chem.* **1979,** *51,* 342.

74. Hu, A.; Dessy, R. E.; Granéli, A. *Anal. Chem.* **1983,** *55,* 320–328.

75. Shulze, G.; Bonigk, W.; Frenzel, W. *Fresenius Z. Anal. Chem.* **1985,** *322,* 225–269.

76. Frenzel, W.; Bratter, P. *Anal. Chim. Acta.* **1986,** *179,* 389–398.

77. Locascio, L. E.; Janata, J. *Anal. Chim. Acta.* **1987,** *194,* 99–107.

78. Schulze, G.; Koschany, M.; Elsholz, O. *Anal. Chim. Acta.* **1987,** *196,* 153–161.

79. Frenzel, W.; Schulze, G. *Analyst.* **1987,** *112,* 133–136.

80. Psaroudakis, S. V.; Efstathiou, C. E. *Analyst.* **1987,** *112,* 1587–1591.

81. Heineman, W. R.; Mark, H. B.; Wise, J. A.; Roston, D. A., in *Laboratory Techniques in Electroanalytical Chemistry;* P. T. Kissinger and W. R. Heineman, Eds.; Marcel Dekker: New York, 1984; p. 156.

82. Danielson, L. G.; Jagner, D.; Josefson, M.; Westerlung, A. *Anal. Chim. Acta.* **1981,** *127,* 147.

83. Hoyer, B.; Kryger, L. *Anal. Chim. Acta.* **1985,** *167,* 11.

84. Froning, M.; Mohl, C.; Ostapczuk, P. *Fresenius J. Anal. Chem.* **1993,** *345,* 233–235.

85. Labar, C. H. *Electrochim. Acta.* **1993,** *38(6),* 807–813.

86. Jagner, D.; Aren, K. *Anal. Chim. Acta.* **1982,** *137,* 201.

87. Fayyad, M. *Electroanalysis.* **1990,** *2,* 631–635.

88. Pheiffer Madsen, P.; Drabaek, I.; Sorensen, J. *Anal. Chim. Acta.* **1983,** *151,* 479–482.

89. Mannino, S. *Analyst.* **1983,** *108,* 1257–1260.

90. Guo, X. *Fenxi Huaxue.* **1983,** *11,* 362–364.

91. Bogoslovskii, V. V.; Gabor Klatsmanyi, P.; Pungor, E. *Magy. Kem. Foly.* **1984,** *90,* 282–284.

92. Pereira-Ramos, J. P.; Chivot, J.; Sarantopoulos, F.; Godard, R. *Analusis.* **1984,** *12,* 249–255.

93. Obiols, J.; Ribera, L. *Afinidad.* **1984,** *November–December,* 513–517.

94. Wang, E.; Sun, W.; Yang, Y. *Anal. Chem.* **1984,** *56,* 1903–1906.

95. Wang, G.; Ma, M.; Yan, J. *Huaxue Xuebao.* **1984,** *42,* 283–287.

96. Wang, Z.; Wang, S. *Fenxi Huaxue.* **1984,** *12,* 796.

97. Mannino, S.; Bianco, M. *J. Micronutr. Anal.* **1985,** *1,* 47–53.

98. Jaya, S.; Prasada Rao, T.; Prabhakara Rao, G. *Talanta.* **1985,** *32,* 1061–1063.

99. Wang, E.; Sun, W. *Anal. Chim. Acta.* **1985,** *172,* 365–370.

100. Zhu, C.; Yan, H. *Huanjing Kexue.* **1985,** *6,* 28–32.

101. Jaya, S.; Rao, T. P.; Rao, G. P. *Bull. Electrochem.* **1986,** *2,* 131–133.

102. Manino, S.; Bianco, M. *Riv. Soc. Ital. Sci. Aliment.* **1986,** *15,* 393–396.

103. McKinnon, A.; Scollary, G. *Analyst.* **1986,** *111,* 589–591.

104. Fayyad, M.; Tutunji, M.; Ramakrishna, R. S.; Taha, Z.H.A. *Analyst.* **1986,** *111,* 471–473.

105. Psaroudakis, S. V.; Efstathiou, E. *Analyst.* **1989,** *114,* 25–28.

106. Wu, G. *Xiamen Daxue Xuebao Ziran Kexueban.* **1986,** *25,* 734–736.

107. Noren, J. G.; Hulthe, P.; Gillberg, C. *Swed. Dent. J.* **1987,** *11,* 45–52.

108. Fayyad, M.; Tutunji, M.; Ramakrishna, R. S.; Taha, Z. *Anal. Lett.* **1987,** *20,* 529–535.

109. Rozali bin Othman, M.; Hill, J. O.; Magee, R. J. *Fresenius Z. Anal. Chem.* **1987,** *326,* 350–353.

110. Fayyad, M. *Anal. Chem.* **1987,** *59,* 209–211.

111. Wang, Y.; Zhang, S. *Fenxi Huaxue.* **1987,** *15,* 31–35.

112. Huang, P. *Fenxi Huaxue.* **1987,** *15,* 574.

113. Wang, Z.; Wang, T. *Zhonghua Yufangyixue Zazhi.* **1987,** *21,* 297–298.

114. Teng, J.; Feng, D.; Zhou, D. *Jinan Liyi Xuebao.* **1988,** *3,* 41–45.

115. Fayyad, M.; Tutunji, M.; Taha, Z. *Anal. Lett.* **1988,** *21,* 1425–1432.

116. Huiliang, H.; Jagner, D.; Renman, L. *Anal. Chim. Acta.* **1988,** *207,* 17–26.

117. Zhou, J.; Yu, X.; Zhang, S. *Gongye Weisheng Yu Zhiyebing.* **1988,** *14,* 15, 29–32.

118. Xiang, Y. *Zhongguo Tiaowiepin.* **1988,** *4,* 28–30.

119. Jin, L.; He, P.; Wu, B. *Fenxi Shiyanshi.* **1988,** *7,* 14–16.

120. Zhou, J.; Zhou, H.; Hu, Y.; Li, D. *Jinan Liyi Xuebao.* **1988,** *3,* 92–94.

121. Yang, P.; Li, D. *Jinan Daxue Xuebao.* **1989,** *1,* 31–36, 59.

122. Huang, P.; Sun, P.; Liu, Y. *Lihua Jianyan Huaxe Fence.* **1989,** *25,* 265–267.

123. Psaroudakis, S. V.; Efstathiou, E.; Hadjiioannou, T. P. *Anal. Lett.* **1989,** *22,* 1753–1763.

124. Sun, X.; Zhang, M.; Guo, S. *Huaxi Yike Daxue Xuebao.* **1989,** *20,* 324–326.

125. Wang, S.; Lin, Q.; Zhou, J.; Feng, D.; Li, D. *Jinan Daxue Xuebao.* **1989,** *1,* 80–81.

126. Xian, Y.; Li, X.; Lian, T.; Zhu, X.; Wang, X. *Gongye Weisheng Yu Zhiyebing.* **1989,** *15,* 226–229.

127. Wang, G.; Li, X.; Zhu, S. *Fenxi Shiyanshi.* **1989,** *8,* 58–59.

128. Zhou, J.; Feng, D.; Li, Y.; Xie, Y. *Jinan Daxue Xuebao.* **1989,** *3,* 52–56.

129. Jin, L.; Su, R.; Fang, Y. *Fenxi Shiyanshi.* **1990,** *9,* 12–15.

130. Zhang, Y.; Han, J. *Zhonghua Laodong Weisheng Zhiyebing Zazhi.* **1990,** *8,* 350–351.

131. Wang, Y. *Shanghai Huanjing Kexue.* **1990,** *9,* 31.

132. Yin, T. *Turang Xuebao.* **1991,** *28,* 108–114.

133. Nanos, C. G.; Karayannis, M. I. *Fresenius J. Anal. Chem.* **1991,** *340,* 253–257.

134. Coetzee, J. F.; Ecoff, J. M. *Anal. Chem.* **1991,** *63,* 957–963.

135. Wang, D.; Liu, H. *Fenxi Huaxe.* **1991,** *19,* 1104.

136. Feng, D.; Zhou, J.; Feng, J.; Chen, J. *Jinan Daxue Xuebao Ziran Kexue Yu Yixueban.* **1991,** *12,* 56–60.

137. Sun, Q.; Hou, S.; Chen, Z.; Zhu, J.; Liu, A. *Fenxi Huaxue.* **1991,** *19,* 1408–1410.

138. Zhang, G.; Wang, S.; Wang, H. *Yejin Fenxi.* **1991,** *11,* 1–3.

139. Zhang, P. *Fenji Ceshi Tongbao.* **1990,** *10,* 50–53.

140. Mannino, S.; Brambilla, M. *Ital. J. Food Sci.* **1992,** *4,* 47–51.

141. Ostapczuk, P. *Clin. Chem.* **1992,** *38,* 1995–2001.

142. Qin, W.; Guo, G.; Zhang, M. *Fenxi Huaxue.* **1992,** *20,* 1361.

143. Suturovic, Z.; Marjanovic, N. *Zito Hleb.* **1992,** *19,* 215–219.

144. Marin, C.; Ostapczuk, P. *Fresenius J. Anal. Chem.* **1992,** *343,* 881–886.

145. Cai, Z.; Qi, D. *Fenxi Huaxe.* **1992,** *20,* 862.

146. Sun, B.; Yang, S. *Huanjing Wuran Yu Fangzhi.* **1992,** *14,* 30–32.

147. Zhou, J.; Mei, Q.; Zhang, S.; Yuan, X. *Gongyye Weisheng Yu Zhiyebing.* **1992,** *18,* 173–176.

148. Jagner, D.; Sahlin, E.; Axelsson, B.; Ratana-Ohpas, R. *Anal. Chim. Acta.* **1993,** *278,* 237–242.

149. Yuan, Y.; Wang, Y.; Gao, C. *Haiyang Yu Huzhao.* **1993,** *24,* 45–50.

150. Cladera, A.; Estela, J. M.; Cerdà, V. *Talanta.* **1990,** *37,* 689–693.